

Extreme Fast Charging of Electric Vehicles: A Technology Overview

Hao Tu, *Student Member, IEEE*, Hao Feng, *Member, IEEE*, Srdjan Srdic, *Senior Member, IEEE*,
and Srdjan Lukic, *Senior Member, IEEE*,

Abstract—With the number of electric vehicles (EVs) on the rise, there is a need for an adequate charging infrastructure to serve these vehicles. The emerging extreme fast charging (XFC) technology has the potential to provide a refueling experience similar to that of gasoline vehicles. In this paper, we review the state-of-the-art EV charging infrastructure, and focus on the XFC technology which will be necessary to support current and future EV refueling needs. We present the design considerations of the XFC stations, and review the typical power electronics converter topologies suitable to deliver XFC. We consider the benefits of using the solid-state transformers (SSTs) in XFC stations to replace the conventional line-frequency transformers and further provide a comprehensive review of medium voltage SST designs for the XFC application.

Index Terms—Charging stations, dc fast charger, electric vehicles, extreme fast charging, solid-state transformer

I. INTRODUCTION

AMID growing concerns about climate change, key government and private stakeholders have pushed for moving away from petroleum as the main energy source for powering our transportation system. Transportation systems powered by electricity can help to reduce the consumption of petroleum: battery electric vehicles (EVs) would be plugged into the grid, and their on-board battery systems can be recharged using clean, renewable electricity.

Moving to an electric transportation model requires battery storage capable of supplying the energy and power demands of the vehicle. Li-ion battery technology has advanced significantly over the last couple of years, making EVs more cost effective and practical. The cost of the batteries has fallen to less than \$120/kWh [1]–[3]. Despite huge improvements in energy density of the Li-ion batteries (200–300 Wh/kg) and the significantly higher efficiency of the electric propulsion drivetrain, the driving range of EVs on one charge is still shorter than the range of the conventional gasoline vehicles due to the orders of magnitude larger (12,000 Wh/kg [2], [4]) energy density of petroleum. In summary, despite the falling cost and major improvement in performance, Li-ion battery degradation at rest and during cycling, charging rate limitations due to the electrochemical processes and limited energy density (compared to petroleum) still pose major challenges to more widespread EV adoption [5], [6].

Beyond Li-ion battery technology limitations, a key remaining challenge for the wide adoption of EVs is the lack of the refueling infrastructure that can quickly and seamlessly recharge EV batteries to extend the driving range during longer trips. Therefore, there is an urgent need for an EV

charging infrastructure that will parallel the existing gasoline stations, particularly in regions where long-distance trips are common. However, designing and deploying such an EV charging infrastructure is complex, and must consider competing industry standards, available technologies, grid impacts, and other technical and policy issues.

In this paper, we first review the state-of-the-art dc fast chargers and present the motivation for and the advantages of grouping dc fast chargers into extreme fast charging (XFC) stations. We review power electronics converter topologies suitable for XFC stations, specifically focusing on AC/DC front-end stage design and isolated and non-isolated DC/DC converter topologies and their applications that satisfy the isolation requirements for automotive traction batteries. Further, we assess the benefits of replacing the conventional line-frequency transformer with the solid-state transformer (SST) in the XFC stations to convert the medium voltage (MV) to low voltage (LV) and provide galvanic isolation. We review the SST topologies for the XFC application proposed in the literature.

II. STATUS OF THE EV CHARGING INFRASTRUCTURE

The Society of Automotive Engineers (SAE) defines conductive charging methods of EVs in North America in SAE J1772 Standard [7]. The ac level 1 and ac level 2 on-board chargers take 120 V and 240 V ac input, respectively, delivering a peak power of 1.9 kW and 19.2 kW, respectively. Due to their relatively low power rating, these on-board chargers are suitable for overnight charging. The limited power ratings of on-board chargers has led to the development of dc fast chargers, typically rated at 50 kW and, more recently, at power levels up to 350 kW. These chargers deliver dc power to the vehicle battery via an isolated power converter located outside the vehicle, and they have the potential to provide EV users with satisfactory charging speed.

Table I summarizes the state-of-the-art dc fast chargers on the market. The state-of-the-art dc fast chargers convert the three-phase ac voltage up to 480 V to the desired dc voltage by two power electronics conversion stages: an AC/DC rectification stage with power factor correction (PFC), which converts three-phase input ac voltage to an intermediate dc voltage; and a DC/DC stage, which converts the intermediate dc voltage into regulated dc voltage required to charge the electric vehicle. The galvanic isolation between the grid and the EV battery can be provided in one of the two following methods. The first option is to use a line-frequency transformer before the AC/DC stage to provide isolation from the grid (See Fig. 1a). The following DC/DC stage is a non-isolated

This work was supported in part by the U.S. Department of Energy, under Award Number DE-EE0008450.

TABLE I: Technical specifications of state-of-the-art dc fast chargers

Manufacturer Model	ABB Terra 53	Tritium Veefil-RT	PHIHONG Integrated Type	Tesla Supercharger	EVTEC espresso&charge	ABB Terra HP
Power	50 kW	50 kW	120 kW	135 kW	150 kW	350 kW
Supported protocols	CCS Type 1 CHAdeMO 1.0	CCS Type 1 & 2 CHAdeMO 1.0	GB/T	Supercharger	SAE Combo-1 CHAdeMO 1.0	SAE Combo-1 CHAdeMO 1.2
Input voltage	480 Vac	380-480 Vac 600-900 Vdc	380 Vac \pm 15% 480 Vac \pm 15%	380-480 Vac	400 Vac \pm 10%	400 Vac \pm 10%
Output voltage	200-500 V 50-500 V	200-500 V 50-500 V	200-750 V	50-410 V	170-500 V	150-920 V
Output current	120 A	125 A	240 A	330 A	300 A	375 A
Peak efficiency	94%	>92%	93.5%	91%	93%	95%
Volume	758 L	495 L	591 L	1047 L	1581 L	1894 L
Weight	400 kg	165 kg	240 kg	600 kg	400 kg	1340 kg
Time to add 200 miles	72 min	72 min	30 min	27 min	24 min	10 min

converter. The second option is to exploit a high-frequency transformer inside an isolated DC/DC converter to provide isolation (See Fig. 1b). If a single-module charger does not meet the power requirement of the dc fast charger system, multiple identical modules are connected in parallel to increase the output power as shown in Fig. 1c and Fig. 1d. An example is the Tesla Supercharger, which is made of 12 paralleled modules [8]. Similar approach is used by most manufacturers listed in Table I.

To ensure compatibility, a number of governing bodies have developed standardized protocols and couplers for dc fast charger system. The five standard dc fast charging systems in use are listed in Table II. The IEC 62196-3 Standard [9] defines four different vehicle coupler configurations for dc fast charging: Configuration AA (proposed and implemented by CHAdeMO Association), Configuration BB (Also known as GB/T and available only in China), Configuration EE (Type 1 Combined Charging System (CCS), adopted in North America) and Configuration FF (Type 2 CCS, adopted in Europe and Australia). There is also a proprietary system developed by Tesla Inc. and used exclusively for Tesla vehicles.

The power delivered to the EV is limited not only by the charge acceptance of the batteries and the ratings of the charger, but also by the connector and cable between the vehicle and the charger. The connector ratings are defined by the standard, and currently the CHAdeMO standard supports the highest power capacity. High charging current requires cables with larger diameters to avoid overheating. The cable weight for 50 kW state-of-the-art fast chargers is about 9 kg [10]. If the battery voltage stays at 400 V level, the cable weight for 200 kW charging can exceed the safety lifting limit for a single person (22.7 kg according to OSHA). One way to reduce the cable weight and deliver more power to the vehicle is to transfer power at higher voltage levels. For 800 V voltage level, the cable weight limits the charging power to be lower than 350 kW [11]. Cable liquid cooling is one potential solution that can effectively reduce the thermal stress on the cable, making smaller and lighter cable feasible for XFC. An alternative might be deploying wireless charging in XFC stations, which eliminates the cable completely. Other advantages of wireless charging include inherent galvanic isolation and convenience. However, wireless charging sys-

tems commonly have a lower efficiency and power density compared to conductive charging systems [12]–[14]. Wireless charging technology review and discussion is beyond the scope of this paper.

III. XFC STATIONS: MOTIVATION, TRENDS AND CHALLENGES

With the market demand for EVs that can cover most travel scenarios on a single charge, most EVs today are able to provide more than 200 miles driving range. Table III shows the battery capacity and driving range for some of the top selling EVs on the market. Given that the vehicle range is acceptable for many driving scenarios, there is a need for a charging infrastructure that can replenish these batteries in a time commensurate with that of the gasoline refueling experience. Assuming energy consumption of 30 kWh per 100 miles, on-board chargers rated at 7.2 kW would require more than 8 hours to add 200 miles range to the EV (assuming the vehicle is charged at constant power). A 50 kW fast chargers still needs more than 1 hour to add 200 miles, while the 135 kW Tesla Supercharger only needs 27 minutes. The recently proposed 350 kW DC ultra-fast chargers can shorten the time of adding 200 miles range to 10 minutes, which is comparable to the refueling experience of gasoline vehicles.

With the EV charging power increasing, designing and building a system that can deliver such high power becomes increasingly challenging and costly. The installation costs of XFC stations can be very high when considering all the necessary electrical service upgrades such as transformer and feeder, condition of the ground surface, conduits from the power source to the service transformer and from the transformer to the fast charger, material costs, permits, and administration. While the installation costs of the dc fast chargers vary from site to site, a significant portion comes from the electrical service upgrades [15]. Consequently, building XFC charging stations with multiple chargers makes more economic sense than building single-port chargers, since some of the site construction overhead is spread over multiple charging ports. With multiple chargers sharing the same upstream equipment, XFC stations' footprint per port can be significantly reduced, allowing for installations in densely populated areas.

With the increasing EV adoption, and ever-increasing charging rates, EVs are likely to become a significant new load

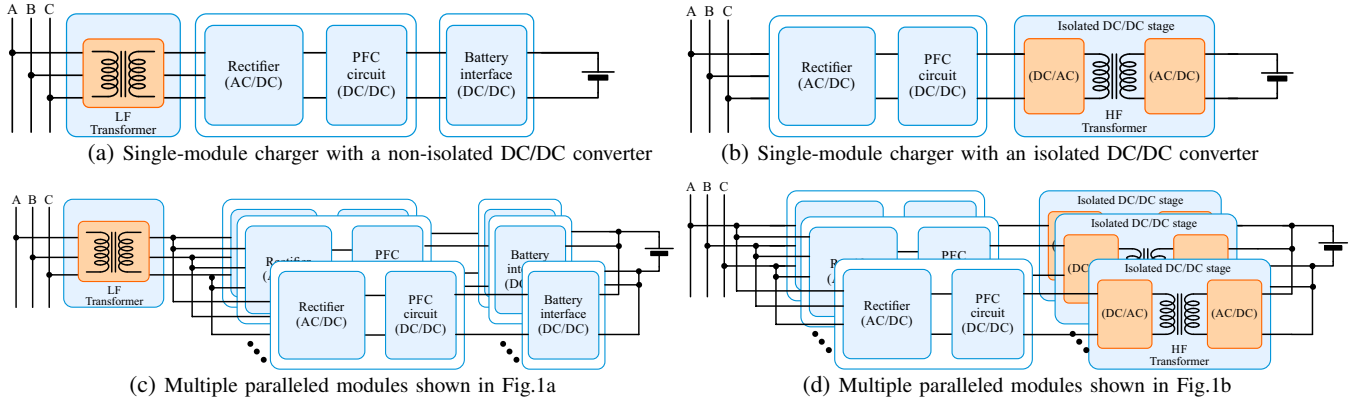


Fig. 1: Simplified block diagram of conventional dc fast charger power conversion systems.

TABLE II: Different standards for DC fast charging systems






Standard	CHAdeMo	GB/T	CCS Type 1	CCS Type 2	Tesla
	IEEE 2030.1.1 IEC 62196-3 (Configuration AA)	GB/T 20234.3 IEC 62196-3 (Configuration BB)	SAE J1772 IEC 62196-3 (Configuration EE)	IEC 62196-3 (Configuration FF)	
Coupler Inlet					
Maximum Voltage	1000 V	1000 V	600 V	1000 V	410 V
Maximum Current	400 A	250 A	200 A	200 A	330 A
Available Power	400 kW	120 kW	150 kW	175 kW	135 kW

TABLE III: EVs on the market and their driving range

Model	Battery Capacity (kWh)	Driving Range (Mile)
Nissan Leaf 62 KWH	62	226
Chevy Bolt EV	60	238
Hyundai Kona Electric	64	258
Tesla Model 3 Long Range	75	310
Tesla Model S 100D	100	370

on the power distribution system and present challenges to the utility. If the EV charging is left uncontrolled, a daily peak load increase and a daily peak load shift due to EV charging may occur, causing transformer and feeder overload, accelerating transformer aging, and increasing power losses [16]–[18]. Further, the chargers' power electronics interface drawing a constant power may have a negative influence on the distribution system stability, cause voltage unbalance and decrease the power quality [19]. One possible method to mitigate the power demand and reduce the impact of EV charging on the grid is to integrate multiple renewable resources and battery energy storage systems into XFC stations [20], [21]. An example is the Tesla supercharger station in Mountain View, California, with 200 kW (400 kWh) of battery energy storage as shown in Fig 2. Smart charging management coordinating multiple EVs in a single XFC charging station or multiple XFC stations can help reduce the peak demand of the XFC installation.

Grouping multiple chargers (thus multiple charging EVs) into an XFC charging station make it possible to schedule vehicle charging and de-rate the station upstream equipment. As the charging power for an EV is a function of the battery size and its state of charge (SOC), the power demand of the charging station can vary significantly when multiple EVs are



Fig. 2: One line diagram of Tesla supercharger station in Mountain View.

charging at the same time. By scheduling the charging of multiple vehicles and exploiting the load diversification resulting from different EV battery capacities and accommodating charge acceptance of the battery as a function of the SOC, the actual system power demand from the grid can be substantially lower than the rated value. If an energy storage system is available at the station, the peak power demand can be further reduced. For example, in [22] the authors show that the power rating of an XFC station with 10 charging slots, each rated at 240 kW, can be set at less than 50% of the rated power, when considering realistic EV arrival times at the station and a realistic distribution of initial EV battery state-of-charge. If a relatively small storage system is connected to the station, more than 98% of the power demand can be satisfied with an average charging delay time of less than 10 s.

In addition to de-rating the upstream grid tie equipment and decreasing the installation cost, significant research focuses on exploiting the diversification effect of the vehicle power requirements of multiple EVs charging simultaneously to achieve different objectives such as demand charge reduction,

charging cost minimization, charging availability improvement, profit maximization, etc. [23], [24]. In [25], a two-stage coordinated charging strategy for EV charging stations is proposed. While the first stage tries to maximize the station's profit and provide as much charging availability as possible, the second stage minimizes the peak demand of the station based on the constraints from the first stage. In [26] an online optimization algorithm is proposed for an EV charging station to minimize the charging cost while constraining the power exchange between the grid and the station. The proposed algorithm allows the EV drivers to opt between a fast charging option to shorten the charging time and a charging option to minimize the cost. Authors in [27] propose an approach to sizing the storage unit for a fast charging station. The approach can reduce the energy cost and storage cost while considering the different driving and charging patterns of EVs. An algorithm proposed in [28] aims at charging multiple EVs to the desired SOC in a given amount of time with the help of vehicle-to-vehicle (V2V) energy transfer. Transferring energy among charging vehicles provides more flexibility in peak demand reduction and cost minimization. However, this requires the chargers in the station to be equipped with bidirectional power flow capability.

In addition to V2V, bidirectional power flow capability enables vehicle-to-grid (V2G) technology implemented in EVs to feed power from the vehicles' batteries to the grid. If properly controlled, the on-board batteries of the EVs can be aggregated into an effective energy storage for the XFC station. Further, the XFC station can also be a coupling point for renewable energy sources (RES) such as solar and wind [29]. Integrating RES and exploiting V2G technology not only adds generation to the station and mitigates demand charges, but also enables profiling the power exchange between the charging station and the grid and therefore provides ancillary services to the grid including load shifting and frequency regulation [30]–[32], reactive power support for voltage regulation [33], [34] and renewable generation firming [35], [36].

Beyond a single station, researchers have looked at utilizing vehicle to infrastructure (V2I) communication, to route EVs to stations that have available capacity, or where their load would present the least stress on the power grid. For example, [37] proposes a publish/subscribe communication framework for EVs, roadside units, and charging stations. The roadside units pass messages between EVs and stations and assist the EVs in locating and reserving the least congested stations. In [38], instead of roadside units, public transportation buses are used as brokers between the message publisher (charging station) and subscriber (EVs) to assist EVs in finding the fastest route to destination. In [39] a power allocation scheme for EV charging stations is proposed. By allocating power to different charging stations and routing EVs, the stations' profitability is increased while providing better quality of service to EV drivers. Another important aspect is the optimal placement of EV charging stations. For example, in [40] the optimal locations and capacities of EV charging stations are determined through a spatial-temporal model of the EV mobility, reducing the planning cost and improving the charger availability.

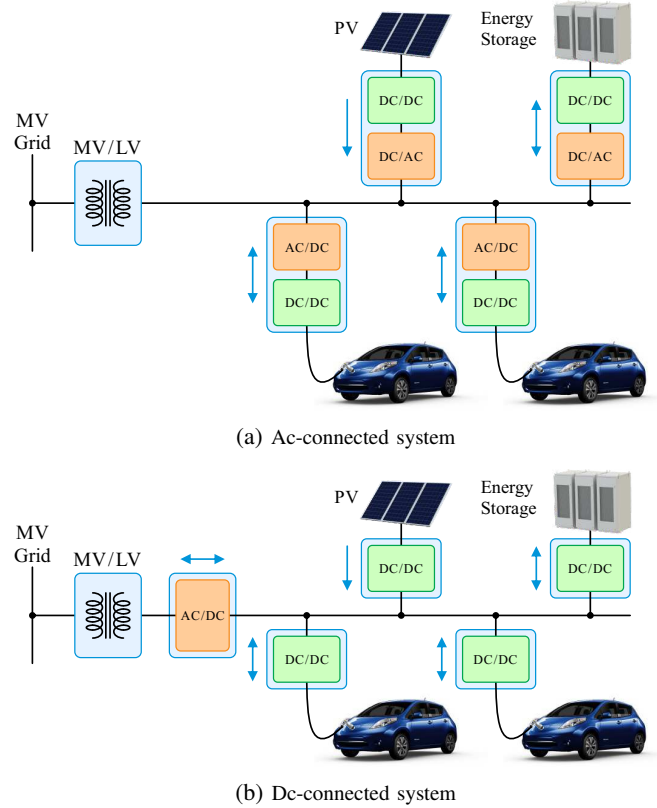


Fig. 3: Configurations for XFC stations.

TABLE IV: Comparison of AC-connected and DC-connected systems

	Ac-connected	Dc-connected
Conversion stages	More	Less
Efficiency	Lower	Higher
front-end de-rating	No	Yes
Control	Complex	Simple
Protection	Straightforward	Complex
Metering	Standardized	Non-standardized

IV. XFC STATION CONCEPTS AND CONVERTER TOPOLOGIES

The local distribution network among multiple chargers, local RES and energy storage can be ac or a dc, as shown in Fig. 3a and Fig. 3b, respectively. Each approach has a number of advantages and challenges as summarized in Table IV. The sections below outline these challenges and opportunities, and review the implementation approaches for both types of charging stations. Different power electronics converters for XFC application are identified and compared. Their advantages and disadvantages are discussed. Topology variations and control improvements proposed in literature to better suit XFC are also discussed. Note that this paper focuses on the converter topologies suitable for XFC application and does not cover the topologies for on-board chargers. Reviews of on-board chargers, integrated chargers, and off-board chargers can be found in [41] and [42].

A. XFC Stations with ac and dc power distribution

For ac-connected systems, a step down-transformer interfaces between the distribution network and a three-phase ac bus operating at 250 V - 480 V line-to-line voltage. The ac bus

supplies each charger at the station, and each charger features a separate AC/DC stage. This approach significantly increases the number of conversion stages between the distribution network and the dc port of the EV or the RES (eg. PV or battery). Having more conversion stages in the ac-connected system increases the system complexity and cost while decreasing the system efficiency. The advantages of using the ac bus include the availability and maturity of the rectifier and inverter technology, availability of ac switchgear and protective devices, and well-established standards and practices for the ac power distribution systems. Further, there are developed standards for EV charging stations such as [43]–[45]. Most state-of-the-art XFC stations are ac-connected systems, for example the Tesla supercharger station in Mountain View, California shown in Fig. 2 and the ABB dc fast charging station in Euroa, Victoria, Australia [46].

For dc-connected systems, one central front-end AC/DC converter is used to create a dc bus, providing a more energy efficient way of interfacing dc energy storage and renewable energy sources. The central front-end features a low-frequency transformer followed by a LV (250 V - 480 V) rectifier stage, or an SST that provides the rectification, voltage step-down and isolation function in a single unit. To accommodate the state-of-the-art battery voltage range (approximately 400 V), the dc bus voltage is normally less than 1000 V. At this voltage level, the design of the XFC stations with a dc bus should comply with the same standards as XFC stations with an ac bus [43]–[45]. Each charger is interfaced to the dc bus with a DC/DC converter, removing the individual AC/DC converters. With a reduced number of conversion stages, the system efficiency is improved compared to that of the ac-connected systems. One potential advantage of the "dc distribution" approach is that there is a single interconnection to the utility through the central front-end. This provides an opportunity to exploit the load diversification resulting from varying EV battery capacities and changing charge acceptance of the battery as a function of the SOC to significantly de-rate the AC/DC converter and the nameplate of the grid connection, thus reducing system installation cost. Other advantages of DC systems include the absence of reactive power in dc systems, which simplifies control [47]. The single inverter interconnection with the grid also simplifies islanding from and connection to the main grid. Another potential advantage of dc distribution systems is the opportunity to use partial power converters to interface between the DC bus and the vehicle [48]–[51]. These partial power converters only process a portion of the power delivered to the vehicle, reducing the converter ratings and thus cost, and improving conversion efficiency. For example, in [50] and [51], different partial power DC/DC converters are proposed to interface to a common dc bus of an XFC station. Since a portion of the power in these converters passes directly from the DC bus to the vehicle, these converters cannot provide galvanic isolation between vehicles. Thus this approach has significant technical hurdles to overcome to meet the relevant charging standards in existence today, which requires that "each output circuit shall be isolated from each other" for an EV charging station [44].

Despite its advantages, a dc-connected system presents

unique challenges such as dc protection and dc metering. While there are available protective devices for LV dc systems including fuses, circuit breakers, solid-state circuit breakers, and protective relays [52], there are no established standards for protection coordination in dc-connected EV charging stations. The protection coordination for dc-connected systems is a complex function of the grounding configuration, fault type, system topology, component specification, size, etc., [53]. This issue becomes even more complicated if the chargers are bidirectional. Because a dc-connected system has limited inertia, it is sensitive to disturbance and might become unstable without fast fault clearance. As a result, the speed of fault detection and isolation is critical to system restoration. Studies on existing dc power distribution systems, such as LV dc microgrids, provide guidelines for protection coordination of dc-connected charging stations. In [54] a protection strategy is presented for a LV dc microgrid considering the coordination between different protective devices. In [55] a protection scheme is proposed for dc systems with a loop-type bus. The proposed scheme is able to detect and isolate the fault and provide power uninterruptedly.

In the dc-connected system, dc meters need to be installed to measure the energy generation and consumption of the RES, battery energy storage and EV chargers. This information is critical for accurate billing of the EV station users and may be used for future station planning [56]. While dc meters are commercially available, there is no established accuracy, calibration, and testing procedures that would allow these units to be used for metering. Developing such a standard and certified dc meters are necessary for the dc-connected systems.

B. Grid-facing AC/DC converters

Grid-facing AC/DC converters provide an interface between the grid and a regulated dc bus. A key performance requirement for these converters is high power quality on the ac and dc sides, achieved by input current shaping and output voltage regulation [57], [58]. In this paper, the AC/DC converters suitable for XFC are identified and shown in Fig. 4. Their features are summarized in Table V. They are further categorized as bidirectional and unidirectional converters.

1) *Bidirectional AC/DC converters*: The most widely used grid-facing AC/DC converter is the three-phase active pulse-width-modulated (PWM) converter with an LCL filter shown in Fig. 4a. This boost-type converter has an output voltage higher than the input line-to-line peak voltage. The six-switch PWM converter generates low harmonic input currents, provides bidirectional power flow, and enables arbitrary power factor (PF) regulation. Due to the simple structure, well-established control schemes, and the availability of low-cost IGBT devices with sufficient current and voltage ratings, this topology is widely adopted in the state-of-the-art dc fast chargers [59].

Another boost-type converter implementation is the neutral-point-clamped (NPC) converter shown in Fig. 4b. This three-level converter enables the utilization of devices with lower voltage ratings that can provide lower switching losses at an acceptable cost. Moreover, the resulting three-level voltage waveform reduces the input current harmonics and dv/dt. In

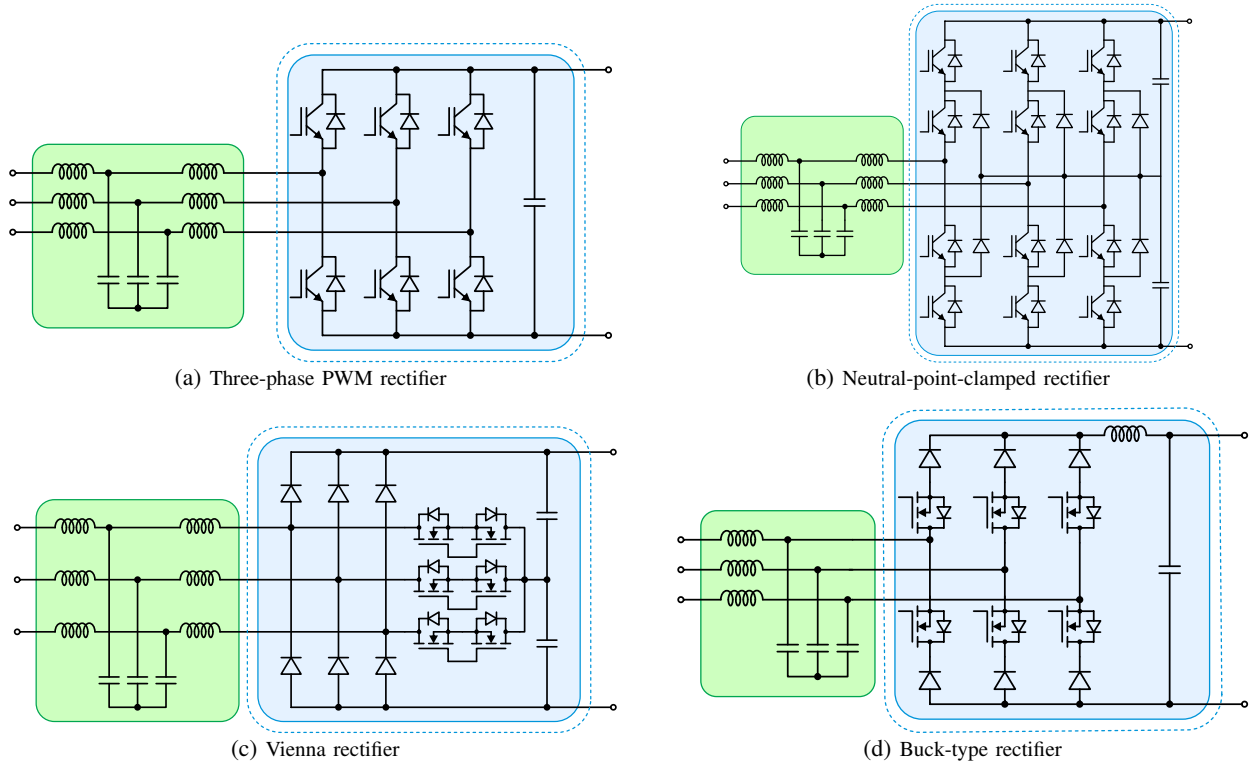


Fig. 4: AC-DC front-end topologies for dc fast chargers.

TABLE V: Comparison of different AC/DC converter topologies for dc fast chargers

Converter	Switches/Diodes	Bidirectional	THD	PF Range	Control Complexity
PWM Converter (Fig. 4a)	6 / 0	Yes	Low	Wide	Low
NPC Converter (Fig. 4b)	12 / 6	Yes	Very Low	Wide	Moderate
Vienna Converter (Fig. 4c)	6 / 6	No	Very Low	Limited	Moderate
Buck-type Converter (Fig. 4d)	6 / 6	No	Low	Limited	Low

[60], a 30 kW EV charger prototype with an NPC front-end achieves low total harmonic distortion (THD) input current with the leakage inductance of input transformer serving as the ac side filter. Another advantage of using NPC converter as the AC/DC front-end is that it explicitly creates a bipolar dc bus [61]. This property is explored in [62] and [63] to implement an EV charging station with a bipolar dc bus, allowing the DC/DC converters to connect to half of the dc bus voltage. The availability of a bipolar dc bus also provides opportunities for partial-power converter implementation for the DC/DC stage; this approach is reviewed in detail in Subsection IV-A.

2) *Unidirectional AC/DC converters*: If only unidirectional power flow is required, the T-type Vienna rectifier, shown in Fig. 4c, is a three-level solution with reduced number of active switches. While it preserves all the advantages of three-level converters, it also shares the common issues of three-level converters including the need for dc-link capacitor voltage balancing. One major limitation for Vienna rectifier is the unidirectional power flow, and limited reactive power control. Due to the restricted modulation vector, the range of achievable reactive power is narrow and depends on the output voltage (the range is $-30^\circ < \phi < 30^\circ$ when the output voltage is higher than twice the peak input ac line-to-line voltage, and it is reduced to $\phi = 0$ if the output voltage is equal to the peak input ac line-to-line voltage). Reference [64] presents

a 25 kW EV charger prototype with a single-switch Vienna rectifier and four parallel three-level DC/DC. In [65], a 20 kW SiC-based Vienna rectifier switching at 140 kHz is 98.6% efficient and features compact passive components. In [66], an EV charger is proposed that uses a Vienna rectifier and two isolated DC/DC converters with each DC/DC converter interfaced to half of the dc bus voltage. By using the DC/DC converters to inject the sixth order harmonic in the dc bus voltage, only one phase of the Vienna rectifier is pulse-width modulated at a time, improving the system efficiency.

If the output voltage is lower than the input line-to-line voltage, a buck-type unidirectional AC/DC converter shown in Fig. 4d can be used. This converter has some advantages over the boost-type topologies, such as inherent short-circuit protection, simple inrush current control, and lower output voltage. An additional advantage is that the input current can be controlled in open-loop. The power flow can be reversed only if the output voltage is reversed. Thus, the converter is only unidirectional with fixed output voltage polarity. The achievable phase difference between the input voltage and the input current fundamental depends on the required output voltage. In order to achieve a higher phase difference, the converter needs to operate with a reduced output voltage range (i.e. if the wide output voltage range is required, the phase shift between the input voltage and input current fundamental

needs to be kept small). The conduction losses are generally higher than for the boost-type converter because more devices are connected in series [67], but the switching losses can be lower. The buck-type converter can still operate at very high efficiency, as reported in [68] where 98.8% efficiency was achieved. In [69], the buck-type rectifier is modified to allow two input phases connecting to each phase leg. With two phase legs conducting the current (in contrast to one phase leg for the buck-type rectifier shown in Fig. 4d), the device conduction loss is reduced while maintaining low THD of the input current. Adding a fourth diode bridge leg connected to the midpoint of the diode bridge and the star-point of the input capacitors leads to reduced voltage stress on the switches [70]. This allows the use of switches with lower voltage rating and better performance, potentially achieving higher system efficiency.

C. Isolated DC/DC converters

A DC/DC converter after the AC/DC front-end provides an interface to the RES, battery energy storage, or the EV battery. Since the electric vehicle's battery must not be grounded (i.e. it must be floating with respect to the ground) at all times, galvanic isolation is required to maintain the isolation between the grid and the battery so that the battery protection remains unaffected by the charging system. This can be achieved by using an isolated DC/DC converter. Isolated DC/DC converter topologies suitable for EV chargers are presented in Fig. 5; their features are summarized in Table VI. A more comprehensive review of isolated DC/DC converters is provided in [71] and [72].

1) *Unidirectional isolated DC/DC converters*: If only unidirectional power flow is required, a possible implementation is the phase-shift full-bridge (PSFB) converter, shown in Fig. 5a. When the converter operates in phase-shift PWM control its active switches operate at zero-voltage switching turn-on (ZVS) [73]. The main disadvantages of this topology are the turn-off losses in the active switches, high losses in the output diodes, and the large ringing across the output diodes due to the LCL resonance of the transformer leakage inductance, parasitic capacitance of the reverse biased diodes and the output inductor. To reduce the voltage overshoot and the ringing, active [73] or passive [74] snubber circuits can be applied at the cost of reduced system efficiency. In [75] and [76], a current-fed PSFB converter is proposed by moving the output inductor to the primary side of the transformer and connecting the diode bridge to an output capacitor directly. This approach minimizes the voltage overshoot and the ringing but the ZVS range becomes highly load-dependent. To maintain ZVS over a wide operating range for EV battery charging, trailing edge PWM is used in [75] while auxiliary circuits are proposed in [76]. Similar auxiliary circuits are used in [77] to achieve ZVS for PSFB converter from no-load to full-load condition of an EV charger.

Another unidirectional isolated DC/DC converter for XFC is the LLC resonant converter, shown in Fig. 5b. Converter output voltage is regulated by changing the switching frequency to adjust the impedance ratio of resonant tank to equivalent load. The LLC converter utilizes the magnetizing current to achieve

ZVS, resulting in low turn-off losses and low transformer losses [78]. The LLC converter can achieve very high efficiency if the input-to-output voltage ratio is narrow [79]. However, it suffers from limited light-load power regulation capability and the ZVS condition may not hold for a wide operating range, thus negatively impacting efficiency.

Multiple approaches are proposed to improve performance for a wide output voltage range and at light load conditions. Various control methods are proposed including PWM, phase-shift, and other hybrid modulation schemes to narrow the range of operating frequency while broadening the output range [80], [81]. In [82], a variable dc voltage is regulated by the AC/DC converter to match the EV battery voltage, allowing the LLC converter to always operate around the resonant frequency with maximum efficiency. Although this method is simple and effective with no extra hardware, wide output voltage range is not guaranteed since the dc voltage variation is limited by the grid voltage and switch voltage rating. Hardware modifications include employing multiple transformers [83] and multiple rectifiers on transformer secondary side [84]. In [85], an extra capacitor paralleled with a four-quadrant switch is inserted in the LLC resonant tank. By modulating the four-quadrant switch, the inserted capacitance and therefore the resonant frequency adapts to the load, improving the efficiency at light-load condition. Despite their effectiveness, these methods require additional hardware and result in higher system cost and larger system volume. Also, a smooth transition between multiple configurations during operation is difficult to achieve.

Another issue for the LLC converter is that the resonant capacitor has to withstand high voltage stress at high power, which complicates component selection. To enhance the power rating and alleviate the stress on switching devices and resonant components, a multilevel LLC converter [86], a three-phase LLC converter [87], and an LLC converter with paralleled modules [88] can be used.

2) *Bidirectional isolated DC/DC converters*: If bidirectional power flow is required, a dual active bridge (DAB) converter (shown in Fig. 5c) can be used for EV charging applications due to its high power density, high efficiency, buck and boost capability, low device stress, small filter components, and low sensitivity to component variation [89]–[96]. When introduced in 1991 [96], the DAB converter was not widely adopted due to the high power losses and relatively low switching frequency of the power semiconductor devices at that time. More recently, the DAB converter started gaining attention, due to the capabilities of the new SiC- and GaN-based power semiconductor devices and the advances in nanocrystalline and amorphous soft magnetic materials, which enabled the converter efficiency and power density improvements [97]. In the DAB converter, the power flow is controlled by adjusting the phase shift between primary and secondary voltage, with transformer leakage inductance serving as the power transfer element. Owing to its simple structure and ZVS operation, the DAB converter has been extensively used in isolated bidirectional DC/DC conversion applications [98], [99].

For EV battery charging, the converter is required to operate with a wide range of voltage gain and power due to the

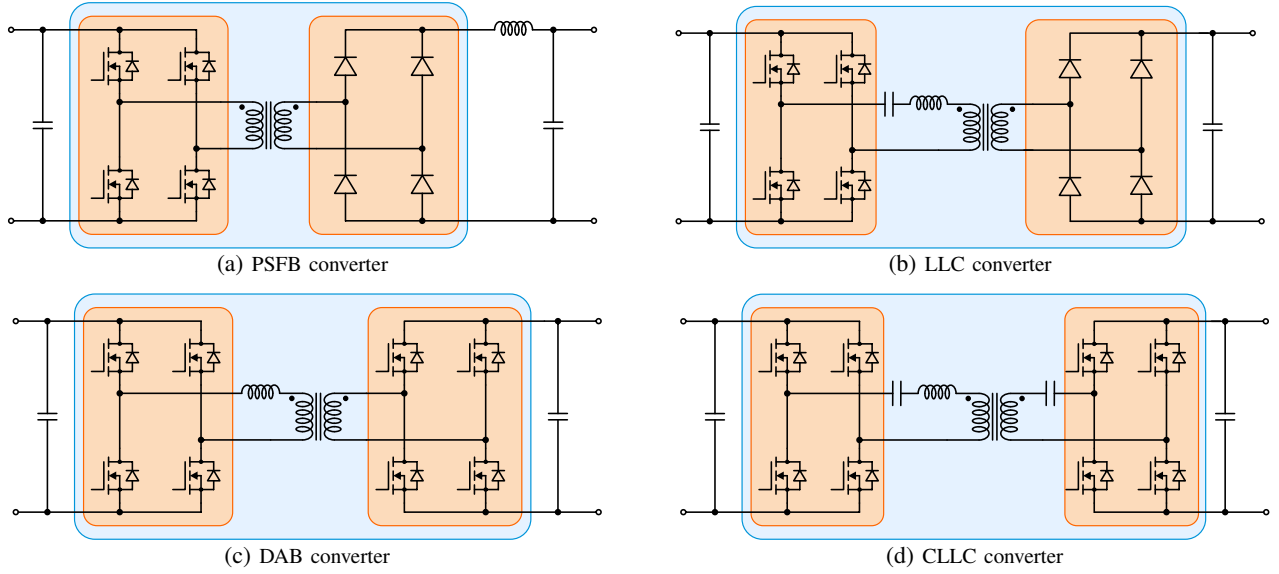


Fig. 5: Isolated DC-DC converter topologies for dc fast chargers.

TABLE VI: Comparison of different isolated DC/DC converter topologies for dc fast chargers

Converter	Switches/Diodes	Bidirectional	Major Advantages and Disadvantages
PSFB converter (Fig. 5a)	4 / 4	No	Simple Control; wide output range. High switching losses in primary switches and output diodes; duty-cycle loss; hard to realize ZVS under light-load.
LLC converter (Fig. 5b)	4 / 4	No	Low reactive current; ZVS on primary side and ZCS on secondary side. Limited controllability; hard to maintain high efficiency and ZVS under wide operating range
DAB converter (Fig. 5c)	8 / 0	Yes	Wide achievable output range. Inherent reactive current; trade-off between reactive power and ZVS condition
CLLC converter (Fig. 5d)	8 / 0	Yes	Low reactive current; wide ZVS range. Limited controllability under wide output range

EV charging profile, under which reactive power can increase dramatically and ZVS condition no longer holds [100]. This causes a dilemma in the design of leakage inductance, in which high leakage benefits a wide ZVS range but worsens the reactive power and results in lower efficiency, and vice versa [101]. To improve the performance under a wide operating range, various modulation schemes have been proposed. In [102], authors propose dual-phase-shift (DPS) modulation to minimize the current-stress of switching devices, where primary and secondary duty cycle are introduced as an additional degrees of freedom. In [103], the DPS is adopted to achieve ZVS under full load range. In [104] and [105], the concept of DPS is further extended to triple-phase-shift (TPS) to enable more degrees of freedom and achieve multiple design objectives such as broader ZVS range, lower current stress, and improved efficiency. In addition, hybrid modulation incorporates operating frequency and pulse density to regulate the transferred power without sacrificing ZVS while controlling the reactive power flow [106], [107]. Recent work in [108] applies TPS to enhance light-load efficiency while switching to DPS to reduce the circulating current under medium- and heavy-load conditions. However, all proposed control strategies have inherent performance trade-offs, and

require complex modulation schemes that may be difficult to implement and may not be as robust to parameter variation. Another concern is the high frequency charging ripple resulting from the reactive power that is inherent to DAB converter operation [94].

Another variant of the bidirectional DC/DC converter is the CLLC converter shown in Fig 5d [109], [110]. Due to its symmetrical circuit, the CLLC converter provides the same voltage gain characteristic in both power flow directions, which reduces the control complexity and facilitates power regulation. Moreover, the CLLC converter distributes two resonant capacitors on both sides of the transformer, which helps reduce the resonant capacitor voltage stress compared to the LLC converter [111]. Compared with the DAB converter, the leakage inductance required for the CLLC resonant tank is much smaller. As a result, the reactive power circulating in the converter is also smaller. Further, the sinusoidal resonant current of the CLLC converter exerts smaller stress on the high-frequency transformer than the DAB converter [112]. However, due to its similarities to the LLC converter, the CLLC converter exhibits similar design trade-offs as the LLC converter such as the ZVS condition and efficiency degradation for a wide voltage and power operating range. The controlla-

bility of CLLC converter is another challenge, as the voltage gain curve against frequency tends to be steady in specific frequency ranges [109]. To solve above issues, authors in [113] add an auxiliary transformer to help realize full load range ZVS while improving power regulation. A detailed parameter design methodology is provided in [114] to realize robust power regulation with a wide operating range. In [115], authors present a design procedure that handles wide voltage gain requirements and integrated magnetic components are used to improve the power density.

In many cases, there is a desire to minimize the number of active devices in a topology. One way to achieve this is to utilize half-bridge equivalents of the converters shown in Fig. 5 including the widely used half-bridge LLC converter [116], [117] and dual half-bridge (DHB) converter [118]–[120]. The half-bridge converters use only four active switches which reduces the cost. Comparing with the full-bridge version, the voltage applied is half of the dc link voltage. This feature is beneficial for the high-frequency transformer design when used in MV applications. However, the current stress on the active devices is doubled, and the degrees of freedom available for converter control are reduced.

D. Non-isolated DC/DC converters

If the charging system is designed to exploit the isolation provided by a different power conversion stage of the XFC system (for example the line-frequency transformer before the AC/DC front-end), a non-isolated DC/DC converter can be used instead of an isolated one, while still providing a floating power supply to the vehicle battery. In this discussion, we consider bidirectional non-isolated DC/DC converters for two reasons. First, the achievable efficiency of bidirectional converters is higher than the unidirectional ones due to synchronous rectification. Second, unlike isolated DC/DC converters, the bidirectional operation does not add more complexity to the control of non-isolated DC/DC converters. Although focusing on the bidirectional converters, the discussions also apply to corresponding unidirectional versions.

Considering the battery voltage is lower than the output voltage of the AC/DC front-end in most cases, a boost converter (from the battery point of view) in Fig. 6a is the simplest non-isolated topology to interface with the battery. The power rating of this converter is limited since the current is carried by a single switch. Also, the inductor size is large if the current ripple needs to be small.

To increase the current carrying capability and reduce the current ripple seen by the battery, two or more phase legs can be interleaved to form a multi-phase interleaved boost converter. Fig. 6b shows an interleaved boost converter with three phase legs. Due to its simple structure, good performance, and scalability to high power, this topology has been widely explored in literature for EV charging application [59], [60], [121]–[123]. In [60], an EV charger prototype is reported to have six phase legs connected in parallel and interleaved to reach 30 kW. In [122], a 100 kW three-phase interleaved boost converter is designed to work in discontinuous conduction mode (DCM). The inductors are small enough to allow both positive and negative current in one switching period, achieving ZVS for all switches. With an optimized inductor design,

the system size can be reduced and efficiency improved. In [123], an interleaved boost converter implementation operating in DCM utilizes the partial power concept by separating the bus voltage into two parts in series. With the converter connecting to part of the bus voltage, switches with lower voltage ratings can be used, potentially reducing losses. The drawback of this method is the extra hardware and control effort to balance the two DC bus voltages.

Another topology that offers better harmonic performance than the boost converter is the three-level boost converter [124] and its bidirectional version [125] as shown in Fig. 6c and Fig. 6d, respectively. The current ripple in the three-level boost converter is only one fourth of that in the boost converter if the same inductor is used, which implies a smaller inductor can be used to meet the current ripple specifications. In [126], the performance of a boost converter, a two-phase interleaved boost converter and a three-level boost converter are compared. The work shows that the three-level boost converter can increase efficiency and reduce the size of the magnetic components. However, the three-level boost converter has high electromagnetic interference (EMI) in terms of common mode noise, which could have a negative impact on the battery system. Further, the three-level boost converters cannot be paralleled easily. If there is a phase shift between paralleled three-level boost phase legs, large circulating currents will result unless interphase inductors are used between phase legs. For high power applications when multiple parallel phase legs are necessary, circulating currents can be suppressed by either switching the phase legs synchronously [127], which eliminates the inductor size reduction due to interleaving, or by using an integrated inductors that suppresses the circulating currents [128]. Due to its three-level nature, the three-level boost converter is suitable for interfacing the EV battery with a bipolar bus such as the EV charging station topologies proposed in [22], [129] and [130].

Another potential three-level topology for fast chargers is a flying capacitor converter shown in Fig. 6e. This three-level topology allows for the use of a smaller inductor compared to a boost converter. Also, the power rating of the converter can be easily increased by paralleling and interleaving multiple phase legs. However, the short circuit protection design is challenging due to the presence of the flying capacitor. In addition, the switching commutation loop of the flying capacitor converter involving the uppermost and lowermost devices is larger than that of boost converter and three-level boost converter [131], which may cause undesired voltage overshoot during switching. In [132], a 55 kW flying capacitor converter prototype boosts the battery voltage three times to the traction inverter bus voltage. The efficiency is above 96.5% over the entire power range. However, to the authors' best knowledge, currently no proposed or implemented dc fast charger uses the flying capacitor converter.

V. SST-BASED MEDIUM VOLTAGE EXTREME FAST CHARGERS

The state-of-the-art fast charging stations are supplied from three-phase low-voltage distribution grid, using up to 480 V

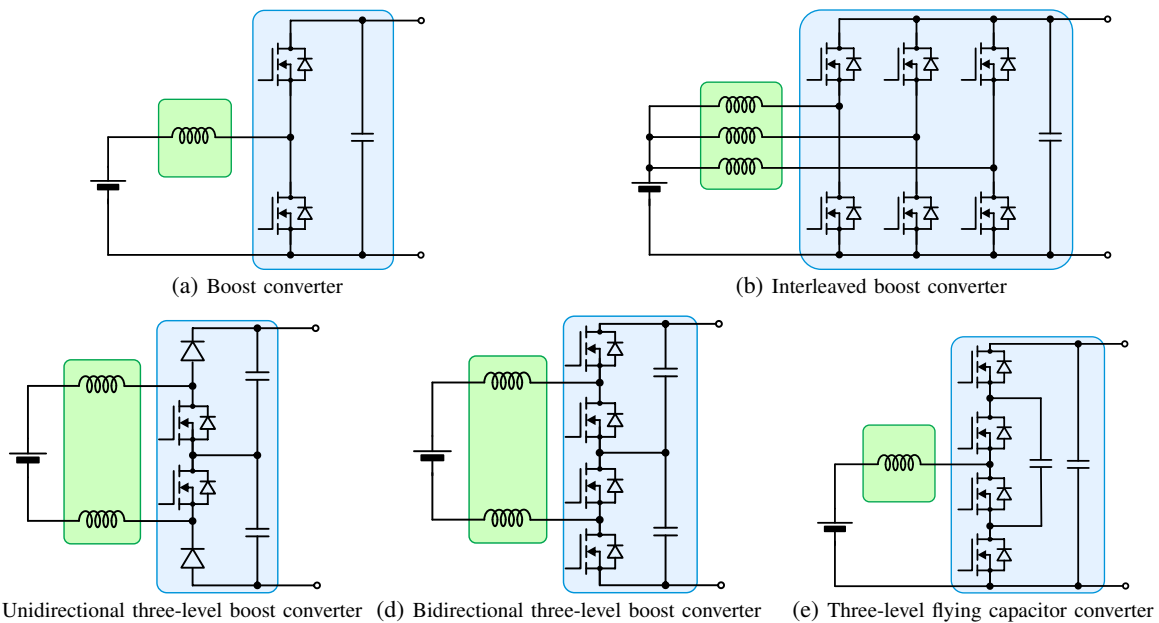


Fig. 6: Non-isolated DC-DC converter topologies for dc fast chargers.

TABLE VII: Comparison of different non-isolated DC/DC converter topologies for dc fast chargers

Converter	Switches/Diodes	Major Advantages and Disadvantages
Boost converter (Fig. 6a)	2 / 0	Simple control. Limited current and voltage capability.
Interleaved boost converter (Fig. 6b)	6 / 0	Increased current capability; low current ripple; simple control; good scalability. Limited voltage capability.
Three-level boost converter (Fig. 6d)	4 / 0	Increased voltage capability; reduced current ripple. Not for interleaving due to circulating current.
Flying capacitor converter (Fig. 6e)	4 / 0	Increased voltage capability; good scalability. Difficult short-circuit protection.



Fig. 7: Comparison of the state-of-the-art dc fast charger station to the SST-based solution. Both stations are rated at 675kW.

line-to-line (depending on the region) as an input. This voltage is typically generated by a dedicated MV-to-LV service transformer. The bulky service transformer increases the size and cost of the system while adding complexity to the installation. To eliminate the need of the MV-to-LV transformer, a power electronics based solid-state transformer (SST) can be used to interface the MV grid directly. The term solid-state transformer (SST) has been loosely used to refer to the concept of replacing line-frequency transformers with power electronics converters that provide voltage conversion and galvanic isolation using high-frequency transformers. Compared to the traditional line-frequency transformer, the SST has a number of unique features such as better controllability, current limiting capabilities, and higher efficiency at light load [133]. Many SSTs proposed

in literature convert the MV ac input to an LV ac output by three conversion stages. The first stage is an active front-end that rectifies the line-frequency MV ac input into dc voltage. Then, an isolated DC/DC stage converts the dc voltage to create a dc bus at a desired voltage level while providing galvanic isolation. The final stage inverts the dc voltage into line-frequency LV ac output. Although other designs such as the single-stage SST proposed in [134] is possible, the three-stage design explicitly creates a dc bus that can interface PVs, battery energy storage systems, EVs and other dc sources and loads [135], [136]. SST topologies and implementations are summarized and compared in [137] and [138].

In the context of XFC, the SST converts the MV ac voltage to LV dc voltage while providing galvanic isolation

by using a high-frequency transformer inside the SST. As the operating frequency of the high-frequency transformer is much higher than the service transformer (tens of kHz versus line frequency), the size of the high-frequency transformer is much smaller than that of the service transformer. Replacing the traditional low frequency transformer and rectifier with an SST provides higher conversion efficiency and significant space savings compared to the state-of-the-art approach. The higher efficiency leads to power savings for the infrastructure owner that can be passed on to the EV owner. The reduced system footprint provides better utilization of the charging station site. This becomes increasingly important as the charging capabilities of the EV batteries improve, and the penetration of EVs increases. A comparison of the state-of-the-art dc fast charger station (based on a Tesla Supercharger station design) to the SST-based solution in Fig. 7 shows the SST-based station has a much smaller footprint for the same power rating.

A. SST Designs for EV charging applications

Although many SST implementations have been proposed in the literature, this paper focuses on systems that are specifically designed for the XFC application, in which they provide rectification, voltage step-down, and isolation function. Most SST-based MV dc fast chargers proposed in literature are implemented as single-phase single-port units that connect directly to EVs. However, they can also serve as the central AC/DC front-end in a dc-connected XFC station with adequate modifications. Further, three-phase implementations can be realized by connecting three identical single-phase converters in delta or wye form.

SSTs commonly use identical modules as building blocks to reach the desired voltage and power levels. To interface to the MV grid directly, the modules are connected in series at the input to increase the voltage blocking capability while the outputs of the modules are connected in parallel to provide large output current at the desired low dc voltage. Fig. 8a shows the MV fast charger topology developed by Electric Power Research Institute (EPRI) and Virginia Tech [139], [140]. Three modules are connected in series at the MV ac side (2.4 kV) and in parallel at the battery side. Each module has an unidirectional NPC AC/DC front-end to realize AC/DC conversion and power factor correction. The internal bus of each module operates at 1250 V allowing off-the-shelf silicon IGBTs or SiC MOSFETs to be used. Following the unidirectional NPC AC/DC front-end, two input-series-output-parallel phase shift full-bridges convert the internal dc bus voltage to the desired output voltage. One demerit of this topology is that it uses a large number of active switches which increases the system cost and limits the achievable efficiency and compactness. Further, the output of the phase shift full-bridges is fixed at 450 V. If the converter is connected to an EV, an additional DC/DC stage is necessary to follow the battery charging profile. In the design, a six-phase interleaved boost converter (from the battery point of view) is used to integrate the EV battery. The system efficiency is close to 96% at 38 kW.

Fig. 8b shows the topology proposed in [141]. Eight modules are connected in series at the MV side to share 8 kV ac voltage. The AC/DC front-end of each module has an uncon-

trolled diode bridge rectifier followed by two unidirectional three-level boost converter phase legs in parallel. The internal bus is 1.4 kV. The DC/DC stage is two input-series-output-parallel half-bridge LLC converters capable of soft-switching. To achieve high efficiency, the LLC converters operate in open loop with 100% duty cycle while the output voltage is regulated by the AC/DC front-end adjusting the bus voltage. This control strategy leads to a narrow output voltage range that may not be able to meet the EV charging profile. If connected directly to an EV, a subsequent DC/DC converter is necessary to accommodate the battery voltage. The system efficiency is about 97.5% at rated load of 25 kW.

At North Carolina State University a 50 kW MV fast charger is developed based on the topology shown in Fig. 8c [142], [145]–[147]. Three modules are connected in series at the MV side to share 2.4 kV ac voltage. Instead of having a diode bridge for each module as in the design in Fig. 8b, a single diode bridge is used to rectify the MV ac input. This reduces the forward voltage drop on diodes and improves the efficiency. Each module has three-level boost converter for power factor correction. The following DC/DC stage consists of a half-bridge NPC converter, a high-frequency transformer and a diode bridge rectifier. The use of the half-bridge NPC converter in the DC/DC stage further reduces the size of the high-frequency transformer. The system efficiency is higher than 97.5% at 50 kW.

Another SST implementation [143], shown in Fig. 8d, uses a full-bridge AC/DC front-end and a dual half-bridge converter in the DC/DC stage. To integrate energy storage into the charging station, a non-isolated boost converter is added between the AC/DC front-end and the DC/DC stage. Compared with the previous converters, this converter is capable of bidirectional power flow but uses more active switches, which results in poor switch utilization and low efficiency. Also, the control is more complex than that of the unidirectional converters. The proposed design is only verified on a down-scaled prototype with 140 V ac input voltage. Similar design using full-bridge converter as the active front-end and current-fed DAB converter as the isolated DC/DC stage can be found in [148]. However, the design from [148] is also verified only at reduced input voltage. In [149], an SST with full-bridge converter as active front-end and DAB converter as the isolated DC/DC stage is constructed with silicon IGBTs. The converter is verified with 3.6 kV input and the reported efficiency is less than 92%.

Another SST implementation led by Delta Electronics aims at building a three-phase SST-Based 400 kW XFC connected to 4.8 kV or 13.2 kV MV grid [144]. The proposed topology is shown in Fig. 8e. Each module is rated at 15 kW with 1 kV ac input voltage. Considering line-to-neutral voltage, three modules are connected in series for 4.8 kV and nine modules for 13.2 kV grid. The AC/DC front-end uses a full-bridge NPC converter while the isolated DC/DC stage is an LLC converter. The primary side of the LLC converter is a three-level converter which reduces the stress on the resonant components. The secondary side is an active full-bridge that can operate in synchronous rectification to reduce the losses. The dc output of the LLC converter is constant 1 kV and a

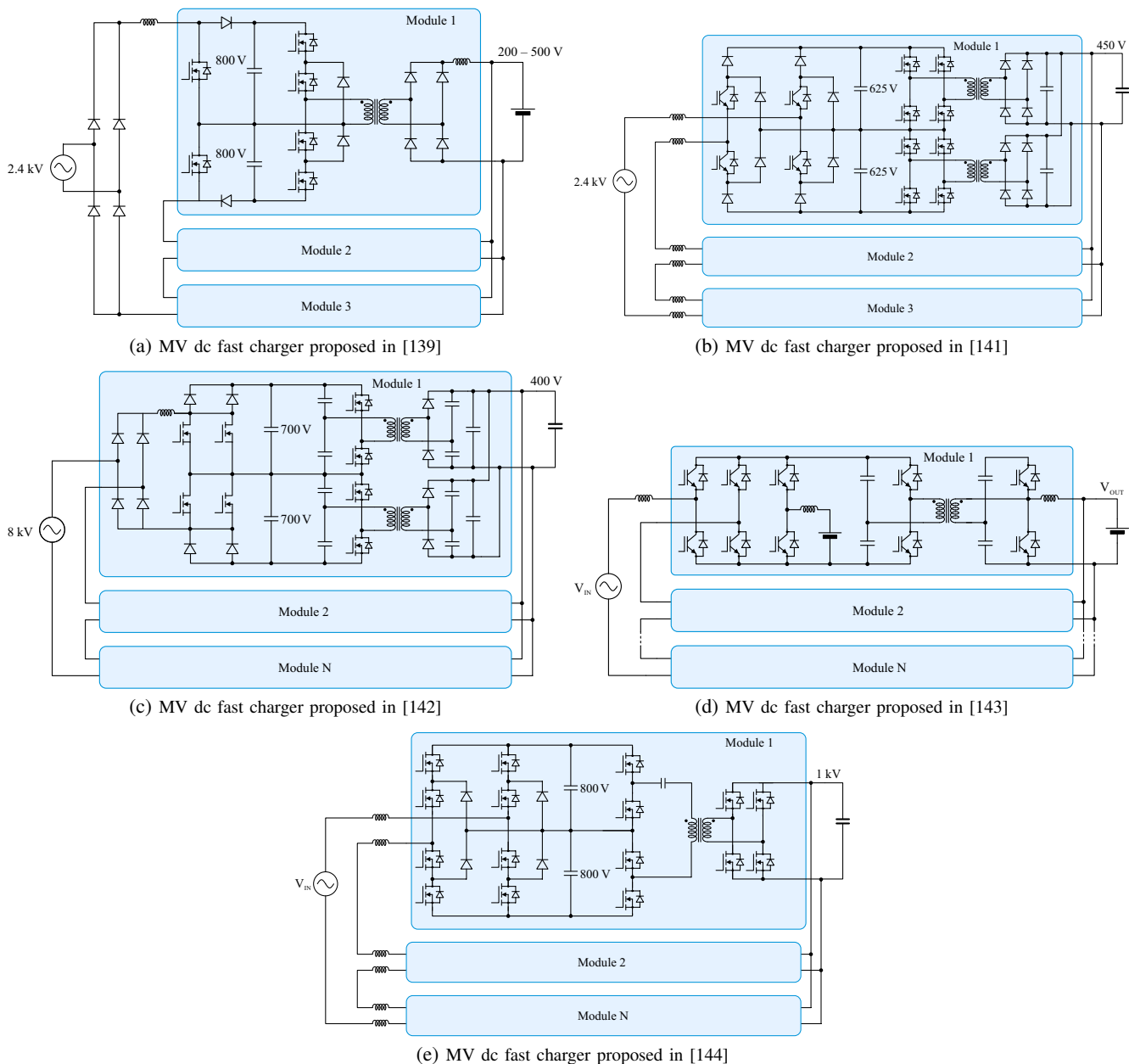


Fig. 8: MV dc fast chargers based on modular SSTs.

subsequent non-isolated DC/DC converter is used to interface the EV battery. All the switches are SiC MOSFETs, which increases the system efficiency but results in higher cost. Bidirectional operation is possible but requires sophisticated control due to the use of the LLC converter. The efficiency of a single module is 97.3% measured at 15 kW and 1 kV ac input.

The modular design with input-series-output-parallel configuration makes the XFC MV-ready by using only low voltage MOSFETs or IGBTs. Redundancy can be achieved by adding more modules. In addition, the multilevel waveform generated by the modular AC/DC front-end presents the potential to reduce the size of the passive filters. However, with modular design, the large number of components can increase the size of the system, offsetting the advantage brought by smaller passives. The input series connection implies that balanced

voltage sharing between modules needs to be maintained. The increase in the control complexity and the number of components may lead to lower system reliability.

B. Single-Module Design

The recent advances in high-voltage SiC MOSFETs with blocking voltages of 10-15 kV enable interfacing MV grid directly by using a single-module converter. This significantly reduces the complexity of the system and has the potential of achieving higher system reliability and efficiency.

In [150], a single-module 10 kW SST is designed and implemented to interface 3.6 kV MV ac input based on 13 kV SiC MOSFETs and junction barrier schottky (JBS) diodes as shown in Fig. 9a. The internal dc bus voltage is 6 kV. To reduce switching losses of the AC/DC front-end, a unipolar modulation with one leg operating as unfolding bridge with line-frequency is used. In addition, the switching frequency of

TABLE VIII: Comparison of different MV dc fast chargers

Topology	Switches/Diodes/Transformers in One Module	Major Advantages and Disadvantages
[139] (Fig. 8a)	12 / 16 / 2	Modular design. Poor switch utilization; unidirectional. fixed output.
[141] (Fig. 8b)	8 / 12 / 2	Modular design; good switch utilization; high efficiency. Narrow output range; unidirectional operation; fixed output.
[142] (Fig. 8c)	$6 / 8 + \frac{4}{3} / 1$	Best switch utilization; compact design; high efficiency; wide output range Not modular design; unidirectional operation.
[143] (Fig. 8d)	10 / 0 / 1	Modular design; bidirectional operation. Very poor switch utilization; low efficiency; complex control.
[144] (Fig. 8e)	16 / 4 / 1	Modular design; (potential) bidirectional operation. Poor switch utilization; complex control; high cost; fixed output.

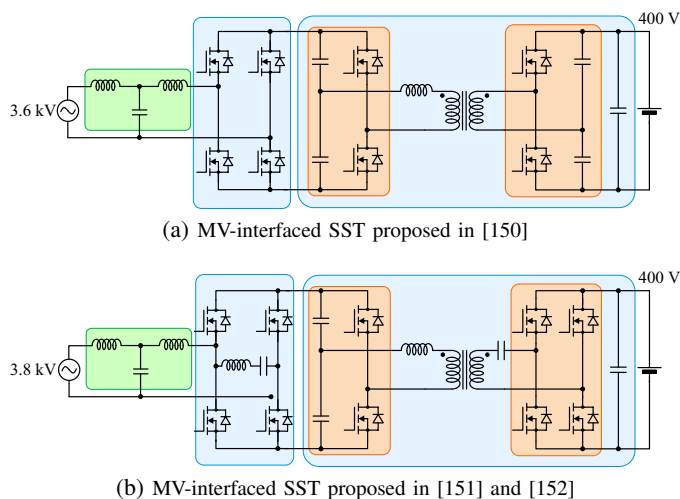


Fig. 9: MV dc fast chargers based on single-module SST technology.

the PWM leg is limited to 6 kHz to further reduce the losses. The isolated DC/DC stage is a DHB converter with 13 kV SiC MOSFETs on the primary side. Phase shift control is used to regulate the output voltage and zero voltage turn-on is achieved for all MOSFETs. The high-frequency transformer with turns ratio of $N = 15$ converts the MV to LV at the secondary side. The measured efficiency at 10 kW was 94%.

In [151] and [152], another single-module SST with larger power rating is designed and implemented to interface 3.8 kV MV ac input to 400 V dc bus based on 10 kV SiC MOSFETs as shown in Fig. 9b. The AC/DC front-end is a full-bridge rectifier with 7 kV internal bus. Similar to [150], a unipolar modulation is adopted for the AC/DC front-end to reduce switching losses. The switching frequency of the PWM leg varies from 35 to 75 kHz. To enable such a high switching frequency at MV, soft-switching over the whole line period is achieved by inserting an LC-branch between the terminals of the two phase legs. The isolated DC/DC stage is an LLC resonant converter with 13 kV SiC MOSFETs half-bridge on the primary side of the high-frequency transformer. The LLC stage operates at a fixed frequency, and the output voltage is regulated by adjusting the internal bus voltage through the AC/DC front-end; ZVS is achieved for all MOSFETs. The system efficiency was measured to be 98% at 25 kW.

It is important to point out that power electronics converters interfaced directly with the MV grid as in the case of the SST,

are subject to relevant protection, safety and power quality standards for MV equipment [153]–[156] in addition to the current standards for EV chargers such those developed by CHAdeMo, IEC, SAE [7], [9], [43]–[45]. Connecting power electronics to the medium voltage line introduces a number of issues in terms of safety and protection that need careful mitigation for the successful adoption of this technology.

VI. CONCLUSION

Despite the increasing number of EVs on the road, the lack of charging infrastructure and long charging times restrict the use of these vehicles to daily commutes and short-distance trips. To address this problem, there is a need for a cost-effective and ubiquitous charging infrastructure that can compete with the existing gasoline-powered vehicle refueling infrastructure.

This paper reviews the state-of-the-art XFC converter technology for EVs that can address the challenges and utilize the opportunities brought by the increasing penetration of EVs. An emerging trend is to co-locate multiple XFCs to form XFC charging stations and thus reduce the installation cost per charging stall. By exploiting the load diversification resulting from different EV battery capacities and different charge acceptance a function of the battery SOC, the installation and operation cost can be reduced, bringing benefits to the station owner and EV users. Energy storage and RES are integrated as part of the charging stations as a common method to reduce high-demand charges that are incurred during peak power hours. It further enables profiling the power exchange between the charging station and the grid and therefore provides ancillary services to support grid operation.

Two different distribution methods for XFC stations are presented. While the ac distribution method is a mature solution with available components and well-established standards, the dc distribution method presents the potential of achieving lower cost and higher efficiency. The suitable power electronics converters for both methods are reviewed and compared. The major challenge for power electronics converters lies in accommodating the wide output voltage and power range of EV charging profile while maintaining high efficiency and high power density.

While the state-of-the-art dc fast chargers requires MV-to-LV line-frequency transformers, another solution is the SST-based dc fast charger that provides rectification, voltage step-

down, and isolation function in a single unit. The SST-based XFCs provide size reduction and efficiency improvement over the state-of-the-art implementations, which can in turn reduce the installation costs by allowing more power delivery on the same station footprint and maximize operating profit by minimizing the power lost in the conversion process.

REFERENCES

- [1] B. Nykvist and M. Nilsson, "Rapidly falling costs of battery packs for electric vehicles," *Nature climate change*, vol. 5, no. 4, p. 329, 2015.
- [2] Z. P. Cano, D. Banham, S. Ye, A. Hintennach, J. Lu, M. Fowler, and Z. Chen, "Batteries and fuel cells for emerging electric vehicle markets," *Nature Energy*, vol. 3, no. 4, p. 279, 2018.
- [3] IEA. Global ev outlook 2019. [Online]. Available: <https://www.iea.org/publications/reports/globalviewoutlook2019/>
- [4] S. Manzetti and F. Mariasiu, "Electric vehicle battery technologies: From present state to future systems," *Renewable and Sustainable Energy Reviews*, vol. 51, pp. 1004–1012, 2015.
- [5] S. Ahmed *et al.*, "Enabling fast charging—a battery technology gap assessment," *Journal of Power Sources*, vol. 367, pp. 250–262, 2017.
- [6] M. Keyser *et al.*, "Enabling fast charging—battery thermal considerations," *Journal of Power Sources*, vol. 367, pp. 228–236, 2017.
- [7] "Sae electric vehicle and plug in hybrid electric vehicle conductive charge coupler," *SAE J1772*, pp. 1–1, October 2017.
- [8] E. Loveday. Rare look inside tesla supercharger. [Online]. Available: <https://insideevs.com/news/322486/rare-look-inside-tesla-supercharger/>
- [9] "Plugs, socket-outlets, vehicle connectors and vehicle inlets - conductive charging of electric vehicles - part 3: Dimensional compatibility and interchangeability requirements for d.c. and a.c./d.c. pin and contact-tube vehicle couplers," *IEC 62196-3:2014*, pp. 1–1, June 2014.
- [10] A. Yoshida *et al.* Chademo quick charger connector with excellent operability. [Online]. Available: <https://global-sei.com/technology/tr/bn84/pdf/84-05.pdf>
- [11] A. Burnham *et al.*, "Enabling fast charging—infrastructure and economic considerations," *Journal of Power Sources*, vol. 367, pp. 237–249, 2017.
- [12] H. Feng, T. Cai, S. Duan, J. Zhao, X. Zhang, and C. Chen, "An lcc-compensated resonant converter optimized for robust reaction to large coupling variation in dynamic wireless power transfer," *IEEE Transactions on Industrial Electronics*, vol. 63, no. 10, pp. 6591–6601, Oct 2016.
- [13] F. Musavi and W. Eberle, "Overview of wireless power transfer technologies for electric vehicle battery charging," *IET Power Electronics*, vol. 7, no. 1, pp. 60–66, January 2014 .
- [14] D. Patil, M. K. McDonough, J. M. Miller, B. Fahimi, and P. T. Balsara, "Wireless power transfer for vehicular applications: Overview and challenges," *IEEE Transactions on Transportation Electrification*, vol. 4, no. 1, pp. 3–37, March 2018 .
- [15] M. Smith and J. Castellano, "Costs associated with non-residential electric vehicle supply equipment: Factors to consider in the implementation of electric vehicle charging stations," New West Technologies, LLC, Tech. Rep., 2015.
- [16] Q. Wu, A. H. Nielsen, J. Østergaard, S. T. Cha, and Y. Ding, "Impact study of electric vehicle (ev) integration on medium voltage (mv) grids," in *2011 2nd IEEE PES International Conference and Exhibition on Innovative Smart Grid Technologies*. IEEE, 2011, pp. 1–7.
- [17] K. Clement-Nyns, E. Haesen, and J. Driesen, "The impact of charging plug-in hybrid electric vehicles on a residential distribution grid," *IEEE Transactions on Power Systems*, vol. 25, no. 1, pp. 371–380, Feb 2010.
- [18] M. J. Rutherford and V. Yousefzadeh, "The impact of electric vehicle battery charging on distribution transformers," in *2011 Twenty-Sixth Annual IEEE Applied Power Electronics Conference and Exposition (APEC)*, March 2011, pp. 396–400.
- [19] H. Shareef, M. M. Islam, and A. Mohamed, "A review of the state-of-the-art charging technologies, placement methodologies, and impacts of electric vehicles," *Renewable and Sustainable Energy Reviews*, vol. 64, pp. 403–420, 2016.
- [20] C. Capasso and O. Veneri, "Experimental study of a dc charging station for full electric and plug in hybrid vehicles," *Applied energy*, vol. 152, pp. 131–142, 2015.
- [21] D. Sbordone, I. Bertini, B. Di Pietra, M. C. Falvo, A. Genovese, and L. Martirano, "Ev fast charging stations and energy storage technologies: A real implementation in the smart micro grid paradigm," *Electric Power Systems Research*, vol. 120, pp. 96–108, 2015.
- [22] S. Bai, D. Yu, and S. Lukic, "Optimum design of an ev/phev charging station with dc bus and storage system," in *2010 IEEE Energy Conversion Congress and Exposition*, Sep. 2010, pp. 1178–1184.
- [23] J. C. Mukherjee and A. Gupta, "A review of charge scheduling of electric vehicles in smart grid," *IEEE Systems Journal*, vol. 9, no. 4, pp. 1541–1553, Dec 2015.
- [24] S. Rajakaruna, F. Shahnia, and A. Ghosh, *Plug in electric vehicles in smart grids: charging strategies*. Springer, 2014.
- [25] Z. Xu, Z. Hu, Y. Song, Z. Luo, K. Zhan, and J. Wu, "Coordinated charging strategy for pevs charging stations," in *2012 IEEE Power and Energy Society General Meeting*, July 2012, pp. 1–8.
- [26] M. Tabari and A. Yazdani, "An energy management strategy for a dc distribution system for power system integration of plug-in electric vehicles," *IEEE Transactions on Smart Grid*, vol. 7, no. 2, pp. 659–668, March 2016.
- [27] S. Negarestani, M. Fotuhi-Firuzabad, M. Rastegar, and A. Rajabi-Ghahnavieh, "Optimal sizing of storage system in a fast charging station for plug-in hybrid electric vehicles," *IEEE Transactions on Transportation Electrification*, vol. 2, no. 4, pp. 443–453, Dec 2016.
- [28] P. You, Z. Yang, M. Chow, and Y. Sun, "Optimal cooperative charging strategy for a smart charging station of electric vehicles," *IEEE Transactions on Power Systems*, vol. 31, no. 4, pp. 2946–2956, July 2016.
- [29] S. Y. Derakhshandeh, A. S. Masoum, S. Deilami, M. A. S. Masoum, and M. E. Hamedani Golshan, "Coordination of generation scheduling with pevs charging in industrial microgrids," *IEEE Transactions on Power Systems*, vol. 28, no. 3, pp. 3451–3461, Aug 2013.
- [30] F. Koyanagi and Y. Uriu, "A strategy of load leveling by charging and discharging time control of electric vehicles," *IEEE Transactions on Power Systems*, vol. 13, no. 3, pp. 1179–1184, Aug 1998.
- [31] C. D. White and K. M. Zhang, "Using vehicle-to-grid technology for frequency regulation and peak-load reduction," *Journal of Power Sources*, vol. 196, no. 8, pp. 3972–3980, 2011.
- [32] T. Wu, Q. Yang, Z. Bao, and W. Yan, "Coordinated energy dispatching in microgrid with wind power generation and plug-in electric vehicles," *IEEE Transactions on Smart Grid*, vol. 4, no. 3, pp. 1453–1463, Sep. 2013.
- [33] M. Klesler, M. C. Kisackicoglu, and L. M. Tolbert, "Vehicle-to-grid reactive power operation using plug-in electric vehicle bidirectional offboard charger," *IEEE Transactions on Industrial Electronics*, vol. 61, no. 12, pp. 6778–6784, Dec 2014.
- [34] J. Y. Yong, V. K. Ramachandaramurthy, K. M. Tan, and N. Mithulananthan, "Bi-directional electric vehicle fast charging station with novel reactive power compensation for voltage regulation," *International Journal of Electrical Power & Energy Systems*, vol. 64, pp. 300–310, 2015.
- [35] W. Hu, C. Su, Z. Chen, and B. Bak-Jensen, "Optimal operation of plug-in electric vehicles in power systems with high wind power penetrations," *IEEE Transactions on Sustainable Energy*, vol. 4, no. 3, pp. 577–585, July 2013.
- [36] M. Ghofrani, A. Arabali, M. Etezadi-Amoli, and M. S. Fadali, "Smart scheduling and cost-benefit analysis of grid-enabled electric vehicles for wind power integration," *IEEE Transactions on Smart Grid*, vol. 5, no. 5, pp. 2306–2313, Sep. 2014.
- [37] Y. Cao, N. Wang, G. Kamel, and Y. Kim, "An electric vehicle charging management scheme based on publish/subscribe communication framework," *IEEE Systems Journal*, vol. 11, no. 3, pp. 1822–1835, Sep. 2017.
- [38] Y. Cao, Y. Miao, G. Min, T. Wang, Z. Zhao, and H. Song, "Vehicular-publish/subscribe (v-p/s) communication enabled on-the-move ev charging management," *IEEE Communications Magazine*, vol. 54, no. 12, pp. 84–92, December 2016.
- [39] I. S. Bayram, G. Michailidis, M. Devetsikiotis, and F. Granelli, "Electric power allocation in a network of fast charging stations," *IEEE Journal on Selected Areas in Communications*, vol. 31, no. 7, pp. 1235–1246, July 2013.
- [40] X. Dong, Y. Mu, H. Jia, J. Wu, and X. Yu, "Planning of fast ev charging stations on a round freeway," *IEEE Transactions on sustainable Energy*, vol. 7, no. 4, pp. 1452–1461, 2016.
- [41] A. Khaligh and S. Dusmez, "Comprehensive topological analysis of conductive and inductive charging solutions for plug-in electric vehicles," *IEEE Transactions on Vehicular Technology*, vol. 61, no. 8, pp. 3475–3489, Oct 2012.
- [42] M. Yilmaz and P. T. Krein, "Review of battery charger topologies, charging power levels, and infrastructure for plug-in electric and hybrid vehicles," *IEEE Transactions on Power Electronics*, vol. 28, no. 5, pp. 2151–2169, May 2013.

- [43] "Electric vehicle conductive charging system - part 1: General requirements," *IEC 61851-1:2017*, pp. 1–287, February 2017.
- [44] "Electric vehicle conductive charging system - part 23: Dc electric vehicle charging station," *IEC 61851-23:2014*, pp. 1–159, March 2014.
- [45] "Electric vehicle conductive charging system - part 24: Digital communication between a d.c. ev charging station and an electric vehicle for control of d.c. charging," *IEC 61851-24:2014*, pp. 1–63, March 2014 .
- [46] A. Agius. What's involved in the construction of an ultra-rapid electric car charging station? [Online]. Available: <https://www.drivezero.com.au/charging/whats-involved-in-the-construction-of-an-ultra-rapid-electric-car-charging-station/>
- [47] S. Bai and S. M. Lukic, "Unified active filter and energy storage system for an mw electric vehicle charging station," *IEEE Transactions on Power Electronics*, vol. 28, no. 12, pp. 5793–5803, Dec 2013 .
- [48] M. S. Agamy, M. Harfman-Todorovic, A. Elasser, S. Chi, R. L. Steigerwald, J. A. Sabate, A. J. McCann, L. Zhang, and F. J. Mueller, "An efficient partial power processing dc/dc converter for distributed pv architectures," *IEEE Transactions on Power Electronics*, vol. 29, no. 2, pp. 674–686, Feb 2014 .
- [49] W. Yu, J. Lai, H. Ma, and C. Zheng, "High-efficiency dc-dc converter with twin bus for dimmable led lighting," *IEEE Transactions on Power Electronics*, vol. 26, no. 8, pp. 2095–2100, Aug 2011 .
- [50] J. Rojas, H. Renaudineau, S. Kouro, and S. Rivera, "Partial power dc-dc converter for electric vehicle fast charging stations," in *IECON 2017 - 43rd Annual Conference of the IEEE Industrial Electronics Society*, Oct 2017, pp. 5274–5279 .
- [51] V. Mahadeva Iyer, S. Gulur, G. Gohil, and S. Bhattacharya, "An approach towards extreme fast charging station power delivery for electric vehicles with partial power processing," *IEEE Transactions on Industrial Electronics*, pp. 1–1, 2019 .
- [52] S. Augustine, J. E. Quiroz, M. J. Reno, and S. Brahma, "Dc microgrid protection: Review and challenges." Sandia National Lab.(SNL-NM), Albuquerque, NM (United States), Tech. Rep., 2018.
- [53] D. Salomonsson, L. Soder, and A. Sannino, "Protection of low-voltage dc microgrids," *IEEE Transactions on Power Delivery*, vol. 24, no. 3, pp. 1045–1053, July 2009.
- [54] D. M. Bui, S. Chen, C. Wu, K. Lien, C. Huang, and K. Jen, "Review on protection coordination strategies and development of an effective protection coordination system for dc microgrid," in *2014 IEEE PES Asia-Pacific Power and Energy Engineering Conference (APPEEC)*, Dec 2014, pp. 1–10.
- [55] J. Park and J. Candelaria, "Fault detection and isolation in low-voltage dc-bus microgrid system," *IEEE Transactions on Power Delivery*, vol. 28, no. 2, pp. 779–787, April 2013.
- [56] D. Meyer and J. Wang, "Integrating ultra-fast charging stations within the power grids of smart cities: a review," *IET Smart Grid*, vol. 1, no. 1, pp. 3–10, 2018.
- [57] B. Singh, B. N. Singh, A. Chandra, K. Al-Haddad, A. Pandey, and D. P. Kothari, "A review of three-phase improved power quality ac-dc converters," *IEEE Transactions on Industrial Electronics*, vol. 51, no. 3, pp. 641–660, June 2004 .
- [58] J. W. Kolar and T. Friedli, "The essence of three-phase pfc rectifier systems-part i," *IEEE Transactions on Power Electronics*, vol. 28, no. 1, pp. 176–198, Jan 2013.
- [59] D. Aggeler, F. Canales, H. Zelaya-De La Parra, A. Coccia, N. Butcher, and O. Apeldoorn, "Ultra-fast dc-charge infrastructures for ev-mobility and future smart grids," in *2010 IEEE PES Innovative Smart Grid Technologies Conference Europe (ISGT Europe)*, Oct 2010, pp. 1–8.
- [60] T. Kang, C. Kim, Y. Suh, H. Park, B. Kang, and D. Kim, "A design and control of bi-directional non-isolated dc-dc converter for rapid electric vehicle charging system," in *2012 Twenty-Seventh Annual IEEE Applied Power Electronics Conference and Exposition (APEC)*, Feb 2012, pp. 14–21 .
- [61] N. Celanovic and D. Boroyevich, "A comprehensive study of neutral-point voltage balancing problem in three-level neutral-point-clamped voltage source pwm inverters," *IEEE Transactions on Power Electronics*, vol. 15, no. 2, pp. 242–249, March 2000.
- [62] S. Rivera, B. Wu, S. Kouro, V. Yaramasu, and J. Wang, "Electric vehicle charging station using a neutral point clamped converter with bipolar dc bus," *IEEE Transactions on Industrial Electronics*, vol. 62, no. 4, pp. 1999–2009, April 2015.
- [63] L. Tan, B. Wu, V. Yaramasu, S. Rivera, and X. Guo, "Effective voltage balance control for bipolar-dc-bus-fed ev charging station with three-level dc-dc fast charger," *IEEE Transactions on Industrial Electronics*, vol. 63, no. 7, pp. 4031–4041, July 2016 .
- [64] J. Kim, J. Lee, T. Eom, K. Bae, M. Shin, and C. Won, "Design and control method of 25kw high efficient ev fast charger," in *2018 21st International Conference on Electrical Machines and Systems (ICEMS)*, Oct 2018, pp. 2603–2607 .
- [65] S. Chen, W. Yu, and D. Meyer, "Design and implementation of forced air-cooled, 140khz, 20kw sic mosfet based vienna pfc," in *2019 IEEE Applied Power Electronics Conference and Exposition (APEC)*, March 2019, pp. 1196–1203 .
- [66] J. A. Anderson, M. Haider, D. Bortis, J. W. Kolar, M. Kasper, and G. Deboy, "New synergetic control of a 20kw isolated vienna rectifier front-end ev battery charger," in *2019 20th Workshop on Control and Modeling for Power Electronics (COMPEL)*, June 2019, pp. 1–8 .
- [67] T. Nussbaumer, M. Baumann, and J. W. Kolar, "Comprehensive design of a three-phase three-switch buck-type pwm rectifier," *IEEE Transactions on Power Electronics*, vol. 22, no. 2, pp. 551–562, March 2007 .
- [68] A. Stupar, T. Friedli, J. Miniböck, and J. W. Kolar, "Towards a 99% efficient three-phase buck-type pfc rectifier for 400-v dc distribution systems," *IEEE Transactions on Power Electronics*, vol. 27, no. 4, pp. 1732–1744, April 2012.
- [69] B. Guo, F. Wang, and E. Aeloiza, "A novel three-phase current source rectifier with delta-type input connection to reduce the device conduction loss," *IEEE Transactions on Power Electronics*, vol. 31, no. 2, pp. 1074–1084, Feb 2016 .
- [70] J. Lei, S. Feng, J. Zhao, W. Chen, P. Wheeler, and M. Shi, "An improved three-phase buck rectifier topology with reduced voltage stress on transistors," *IEEE Transactions on Power Electronics*, pp. 1–1, 2019 .
- [71] Y. Du, S. Lukic, B. Jacobson, and A. Huang, "Review of high power isolated bi-directional dc-dc converters for phev/ev dc charging infrastructure," in *2011 IEEE Energy Conversion Congress and Exposition*, Sep. 2011, pp. 553–560.
- [72] P. He and A. Khaligh, "Comprehensive analyses and comparison of 1 kw isolated dc-dc converters for bidirectional ev charging systems," *IEEE Transactions on Transportation Electrification*, vol. 3, no. 1, pp. 147–156, March 2017.
- [73] J. Sabate, V. Vlatkovic, R. Ridley, and F. Lee, "High-voltage, high-power, zvs, full-bridge pwm converter employing an active snubber," in *[Proceedings] APEC'91: Sixth Annual Applied Power Electronics Conference and Exhibition*. IEEE, 1991, pp. 158–163.
- [74] Jung-Goo Cho, Ju-Won Baek, Chang-Yong Jeong, and Geun-Hie Rim, "Novel zero-voltage and zero-current-switching full-bridge pwm converter using a simple auxiliary circuit," *IEEE Transactions on Industry Applications*, vol. 35, no. 1, pp. 15–20, Jan 1999.
- [75] D. S. Gautam, F. Musavi, W. Eberle, and W. G. Dunford, "A zero-voltage switching full-bridge dc-dc converter with capacitive output filter for plug-in hybrid electric vehicle battery charging," *IEEE Transactions on Power Electronics*, vol. 28, no. 12, pp. 5728–5735, Dec 2013 .
- [76] M. Pahlevaninezhad, P. Das, J. Drobnik, P. K. Jain, and A. Bakhshai, "A novel zvzcs full-bridge dc/dc converter used for electric vehicles," *IEEE Transactions on Power Electronics*, vol. 27, no. 6, pp. 2752–2769, June 2012 .
- [77] M. Pahlevaninezhad, J. Drobnik, P. K. Jain, and A. Bakhshai, "A load adaptive control approach for a zero-voltage-switching dc/dc converter used for electric vehicles," *IEEE Transactions on Industrial Electronics*, vol. 59, no. 2, pp. 920–933, Feb 2012 .
- [78] Bo Yang, F. C. Lee, A. J. Zhang, and Guisong Huang, "Llc resonant converter for front end dc/dc conversion," in *APEC. Seventeenth Annual IEEE Applied Power Electronics Conference and Exposition (Cat. No.02CH37335)*, vol. 2, March 2002, pp. 1108–1112 vol.2.
- [79] J. E. Huber, J. Miniböck, and J. W. Kolar, "Generic derivation of dynamic model for half-cycle dcm series resonant converters," *IEEE Transactions on Power Electronics*, vol. 33, no. 1, pp. 4–7, Jan 2018.
- [80] I. Lee, "Hybrid dc-dc converter with phase-shift or frequency modulation for nev battery charger," *IEEE Transactions on Industrial Electronics*, vol. 63, no. 2, pp. 884–893, Feb 2016.
- [81] M. Pahlevani, S. Pan, and P. Jain, "A hybrid phase-shift modulation technique for dc/dc converters with a wide range of operating conditions," *IEEE Transactions on Industrial Electronics*, vol. 63, no. 12, pp. 7498–7510, Dec 2016.
- [82] H. Wang, S. Dusmez, and A. Khaligh, "Maximum efficiency point tracking technique for llc-based pev chargers through variable dc link control," *IEEE Transactions on Industrial Electronics*, vol. 61, no. 11, pp. 6041–6049, Nov 2014.
- [83] H. Hu, X. Fang, F. Chen, Z. J. Shen, and I. Batarseh, "A modified high-efficiency llc converter with two transformers for wide input-voltage range applications," *IEEE Transactions on Power Electronics*, vol. 28, no. 4, pp. 1946–1960, April 2013 .

- [84] H. Wu, Y. Li, and Y. Xing, "Llc resonant converter with semiactive variable-structure rectifier (sa-vs) for wide output voltage range application," *IEEE Transactions on Power Electronics*, vol. 31, no. 5, pp. 3389–3394, May 2016.
- [85] Z. Hu, Y. Qiu, L. Wang, and Y. Liu, "An interleaved llc resonant converter operating at constant switching frequency," *IEEE Transactions on Power Electronics*, vol. 29, no. 6, pp. 2931–2943, June 2014 .
- [86] A. Coccia, F. Canales, P. Barbosa, and S. Ponnaluri, "Wide input voltage range compensation in dc/dc resonant architectures for on-board traction power supplies," in *2007 European Conference on Power Electronics and Applications*, Sep. 2007, pp. 1–10 .
- [87] Y. Nakahara, H. Otake, T. M. Evans, T. Yoshida, M. Tsuruya, and K. Nakahara, "Three-phase llc series resonant dc/dc converter using sic mosfets to realize high-voltage and high-frequency operation," *IEEE Transactions on Industrial Electronics*, vol. 63, no. 4, pp. 2103–2110, April 2016 .
- [88] H.-m. Yoon, J.-h. Kim, and E.-h. Song, "Design of a novel 50 kw fast charger for electric vehicles," *Journal of Central South University*, vol. 20, no. 2, pp. 372–377, 2013 .
- [89] M. N. Kheraluwala, R. W. Gascoigne, D. M. Divan, and E. D. Baumann, "Performance characterization of a high-power dual active bridge dc-to-dc converter," *IEEE Transactions on Industry Applications*, vol. 28, no. 6, pp. 1294–1301, Nov 1992.
- [90] Sangtaek Han and D. Divan, "Bi-directional dc/dc converters for plug-in hybrid electric vehicle (phev) applications," in *2008 Twenty-Third Annual IEEE Applied Power Electronics Conference and Exposition*, Feb 2008, pp. 784–789.
- [91] C. Mi, H. Bai, C. Wang, and S. Gargies, "Operation, design and control of dual h-bridge-based isolated bidirectional dc-dc converter," *IET Power Electronics*, vol. 1, no. 4, pp. 507–517, December 2008.
- [92] R. J. Ferreira, L. M. Miranda, R. E. Araújo, and J. P. Lopes, "A new bi-directional charger for vehicle-to-grid integration," in *2011 2nd IEEE PES International Conference and Exhibition on Innovative Smart Grid Technologies*, Dec 2011, pp. 1–5.
- [93] H. van Hoek, M. Neubert, and R. W. De Doncker, "Enhanced modulation strategy for a three-phase dual active bridge-boosting efficiency of an electric vehicle converter," *IEEE Transactions on Power Electronics*, vol. 28, no. 12, pp. 5499–5507, Dec 2013.
- [94] L. Xue, Z. Shen, D. Boroyevich, P. Mattavelli, and D. Diaz, "Dual active bridge-based battery charger for plug-in hybrid electric vehicle with charging current containing low frequency ripple," *IEEE Transactions on Power Electronics*, vol. 30, no. 12, pp. 7299–7307, Dec 2015.
- [95] L. Xue, M. Mu, D. Boroyevich, and P. Mattavelli, "The optimal design of gan-based dual active bridge for bi-directional plug-in hybrid electric vehicle (phev) charger," in *2015 IEEE Applied Power Electronics Conference and Exposition (APEC)*, March 2015, pp. 602–608.
- [96] R. W. De Doncker, D. M. Divan, and M. H. Kheraluwala, "A three-phase soft-switched high power density dc/dc converter for high power applications," in *Conference Record of the 1988 IEEE Industry Applications Society Annual Meeting*, Oct 1988, pp. 796–805 vol.1.
- [97] H. Akagi, T. Yamagishi, N. M. L. Tan, S. Kinouchi, Y. Miyazaki, and M. Koyama, "Power-loss breakdown of a 750-v 100-kw 20-khz bidirectional isolated dc-dc converter using sic-mosfet/sbd dual modules," *IEEE Transactions on Industry Applications*, vol. 51, no. 1, pp. 420–428, Jan 2015.
- [98] J. E. Huber and J. W. Kolar, "Applicability of solid-state transformers in today's and future distribution grids," *IEEE Transactions on Smart Grid*, vol. 10, no. 1, pp. 317–326, Jan 2019.
- [99] N. M. L. Tan, T. Abe, and H. Akagi, "Design and performance of a bidirectional isolated dc-dc converter for a battery energy storage system," *IEEE Transactions on Power Electronics*, vol. 27, no. 3, pp. 1237–1248, March 2012.
- [100] H. Wen, W. Xiao, and B. Su, "Nonactive power loss minimization in a bidirectional isolated dc-dc converter for distributed power systems," *IEEE Transactions on Industrial Electronics*, vol. 61, no. 12, pp. 6822–6831, Dec 2014.
- [101] A. Rodríguez, A. Vázquez, D. G. Lamar, M. M. Hernando, and J. Sebastián, "Different purpose design strategies and techniques to improve the performance of a dual active bridge with phase-shift control," *IEEE Transactions on Power Electronics*, vol. 30, no. 2, pp. 790–804, Feb 2015.
- [102] B. Zhao, Q. Song, W. Liu, and W. Sun, "Current-stress-optimized switching strategy of isolated bidirectional dc-dc converter with dual-phase-shift control," *IEEE Transactions on Industrial Electronics*, vol. 60, no. 10, pp. 4458–4467, Oct 2013.
- [103] G. Oggier, G. O. García, and A. R. Oliva, "Modulation strategy to operate the dual active bridge dc-dc converter under soft switching in the whole operating range," *IEEE Transactions on Power Electronics*, vol. 26, no. 4, pp. 1228–1236, April 2011.
- [104] F. Krismer and J. W. Kolar, "Efficiency-optimized high-current dual active bridge converter for automotive applications," *IEEE Transactions on Industrial Electronics*, vol. 59, no. 7, pp. 2745–2760, July 2012.
- [105] J. Huang, Y. Wang, Z. Li, and W. Lei, "Unified triple-phase-shift control to minimize current stress and achieve full soft-switching of isolated bidirectional dc-dc converter," *IEEE Transactions on Industrial Electronics*, vol. 63, no. 7, pp. 4169–4179, July 2016.
- [106] J. Hiltunen, V. Väisänen, R. Juntunen, and P. Silventoinen, "Variable-frequency phase shift modulation of a dual active bridge converter," *IEEE Transactions on Power Electronics*, vol. 30, no. 12, pp. 7138–7148, Dec 2015.
- [107] G. G. Oggier and M. Ordonez, "High-efficiency dab converter using switching sequences and burst mode," *IEEE Transactions on Power Electronics*, vol. 31, no. 3, pp. 2069–2082, March 2016.
- [108] A. Taylor, G. Liu, H. Bai, A. Brown, P. M. Johnson, and M. McAmmond, "Multiple-phase-shift control for a dual active bridge to secure zero-voltage switching and enhance light-load performance," *IEEE Transactions on Power Electronics*, vol. 33, no. 6, pp. 4584–4588, June 2018.
- [109] W. Chen, P. Rong, and Z. Lu, "Snubberless bidirectional dc-dc converter with new clc resonant tank featuring minimized switching loss," *IEEE Transactions on Industrial Electronics*, vol. 57, no. 9, pp. 3075–3086, Sep. 2010 .
- [110] Z. U. Zahid, Z. M. Dalala, R. Chen, B. Chen, and J. Lai, "Design of bidirectional dc-dc resonant converter for vehicle-to-grid (v2g) applications," *IEEE Transactions on Transportation Electrification*, vol. 1, no. 3, pp. 232–244, Oct 2015 .
- [111] J. Jung, H. Kim, M. Ryu, and J. Baek, "Design methodology of bidirectional clc resonant converter for high-frequency isolation of dc distribution systems," *IEEE Transactions on Power Electronics*, vol. 28, no. 4, pp. 1741–1755, April 2013.
- [112] S. Zhao, Q. Li, F. C. Lee, and B. Li, "High-frequency transformer design for modular power conversion from medium-voltage ac to 400 vdc," *IEEE Transactions on Power Electronics*, vol. 33, no. 9, pp. 7545–7557, Sep. 2018.
- [113] C. Wang, S. Zhang, Y. Wang, B. Chen, and J. Liu, "A 5-kw isolated high voltage conversion ratio bidirectional clc resonant dc-dc converter with wide gain range and high efficiency," *IEEE Transactions on Power Electronics*, vol. 34, no. 1, pp. 340–355, Jan 2019.
- [114] J. Huang, X. Zhang, Z. Shuai, X. Zhang, P. Wang, L. H. Koh, J. Xiao, and X. Tong, "Robust circuit parameters design for the clc-type dc transformer in the hybrid ac-dc microgrid," *IEEE Transactions on Industrial Electronics*, vol. 66, no. 3, pp. 1906–1918, March 2019.
- [115] B. Li, Q. Li, F. C. Lee, Z. Liu, and Y. Yang, "A high-efficiency high-density wide-bandgap device-based bidirectional on-board charger," *IEEE Journal of Emerging and Selected Topics in Power Electronics*, vol. 6, no. 3, pp. 1627–1636, Sep. 2018.
- [116] Peiwen He and A. Khaligh, "Design of 1 kw bidirectional half-bridge clc converter for electric vehicle charging systems," in *2016 IEEE International Conference on Power Electronics, Drives and Energy Systems (PEDES)*, Dec 2016, pp. 1–6.
- [117] C. Zhang, P. Li, Z. Kan, X. Chai, and X. Guo, "Integrated half-bridge clc bidirectional converter for energy storage systems," *IEEE Transactions on Industrial Electronics*, vol. 65, no. 5, pp. 3879–3889, May 2018 .
- [118] F. Z. Peng, Hui Li, Gui-Jia Su, and J. S. Lawler, "A new zvs bidirectional dc-dc converter for fuel cell and battery application," *IEEE Transactions on Power Electronics*, vol. 19, no. 1, pp. 54–65, Jan 2004.
- [119] Hui Li, Danwei Liu, F. Z. Peng, and Gui-Jia Su, "Small signal analysis of a dual half bridge isolated zvs bi-directional dc-dc converter for electrical vehicle applications," in *2005 IEEE 36th Power Electronics Specialists Conference*, June 2005, pp. 2777–2782.
- [120] Danwei Liu and Hui Li, "Design and implementation of a dsp based digital controller for a dual half bridge isolated bi-directional dc-dc converter," in *Twenty-First Annual IEEE Applied Power Electronics Conference and Exposition, 2006. APEC '06.*, March 2006, pp. 5 pp.–.
- [121] O. Garcia, P. Zumel, A. de Castro, and A. Cobos, "Automotive dc-dc bidirectional converter made with many interleaved buck stages," *IEEE Transactions on Power Electronics*, vol. 21, no. 3, pp. 578–586, May 2006.
- [122] J. Zhang, J. Lai, R. Kim, and W. Yu, "High-power density design of a soft-switching high-power bidirectional dc-dc converter," *IEEE*

- Transactions on Power Electronics*, vol. 22, no. 4, pp. 1145–1153, July 2007.
- [123] D. Christen, F. Jauch, and J. Biel, “Ultra-fast charging station for electric vehicles with integrated split grid storage,” in *2015 17th European Conference on Power Electronics and Applications (EPE'15 ECCE-Europe)*, Sep. 2015, pp. 1–11.
- [124] M. T. Zhang, Yimin Jiang, F. C. Lee, and M. M. Jovanovic, “Single-phase three-level boost power factor correction converter,” in *Proceedings of 1995 IEEE Applied Power Electronics Conference and Exposition - APEC'95*, vol. 1, March 1995, pp. 434–439 vol.1 .
- [125] P. J. Grbovic, P. Delarue, P. Le Moigne, and P. Bartholomeus, “A bidirectional three-level dc-dc converter for the ultracapacitor applications,” *IEEE Transactions on Industrial Electronics*, vol. 57, no. 10, pp. 3415–3430, Oct 2010 .
- [126] S. Dusmez, A. Hasanzadeh, and A. Khaligh, “Comparative analysis of bidirectional three-level dc-dc converter for automotive applications,” *IEEE Transactions on Industrial Electronics*, vol. 62, no. 5, pp. 3305–3315, May 2015.
- [127] R. M. Cuzner, A. R. Bendre, P. J. Faill, and B. Semenov, “Implementation of a non-isolated three level dc/dc converter suitable for high power systems,” in *2007 IEEE Industry Applications Annual Meeting*, Sep. 2007, pp. 2001–2008 .
- [128] L. Tan, N. Zhu, and B. Wu, “An integrated inductor for eliminating circulating current of parallel three-level dc-dc converter-based ev fast charger,” *IEEE Transactions on Industrial Electronics*, vol. 63, no. 3, pp. 1362–1371, March 2016 .
- [129] Y. Du, X. Zhou, S. Bai, S. Lukic, and A. Huang, “Review of non-isolated bi-directional dc-dc converters for plug-in hybrid electric vehicle charge station application at municipal parking decks,” in *2010 Twenty-Fifth Annual IEEE Applied Power Electronics Conference and Exposition (APEC)*, Feb 2010, pp. 1145–1151.
- [130] L. Tan, B. Wu, S. Rivera, and V. Yaramasu, “Comprehensive dc power balance management in high-power three-level dc-dc converter for electric vehicle fast charging,” *IEEE Transactions on Power Electronics*, vol. 31, no. 1, pp. 89–100, Jan 2016.
- [131] Z. Zhang, H. Tu, X. She, T. Sadilek, R. Ramabhadran, H. Hu, and W. Earls, “High-efficiency silicon carbide (sic) converter using paralleled discrete devices in energy storage systems,” in *2019 IEEE Energy Conversion Congress and Exposition (ECCE)*, Sep. 2019, pp. 2471–2477.
- [132] W. Qian, H. Cha, F. Z. Peng, and L. M. Tolbert, “55-kw variable 3x dc-dc converter for plug-in hybrid electric vehicles,” *IEEE Transactions on Power Electronics*, vol. 27, no. 4, pp. 1668–1678, April 2012.
- [133] J. W. Kolar and J. E. Huber, “Solid-state transformers-key design challenges, applicability, and future concepts,” in *Conference Guide*. IEEE, 2016, pp. 26–26 .
- [134] Q. Zhu, L. Wang, A. Q. Huang, K. Booth, and L. Zhang, “7.2-kv single-stage solid-state transformer based on the current-fed series resonant converter and 15-kv sic mosfets,” *IEEE Transactions on Power Electronics*, vol. 34, no. 2, pp. 1099–1112, Feb 2019 .
- [135] X. She, A. Q. Huang, S. Lukic, and M. E. Baran, “On integration of solid-state transformer with zonal dc microgrid,” *IEEE Transactions on Smart Grid*, vol. 3, no. 2, pp. 975–985, June 2012 .
- [136] X. Yu, X. She, X. Zhou, and A. Q. Huang, “Power management for dc microgrid enabled by solid-state transformer,” *IEEE Transactions on Smart Grid*, vol. 5, no. 2, pp. 954–965, March 2014 .
- [137] X. She, A. Q. Huang, and R. Burgos, “Review of solid-state transformer technologies and their application in power distribution systems,” *IEEE Journal of Emerging and Selected Topics in Power Electronics*, vol. 1, no. 3, pp. 186–198, Sep. 2013 .
- [138] A. Q. Huang, “Medium-voltage solid-state transformer: Technology for a smarter and resilient grid,” *IEEE Industrial Electronics Magazine*, vol. 10, no. 3, pp. 29–42, Sep. 2016 .
- [139] EPRI, “Utility direct medium voltage dc fast charger update: Dc fast charger characterization,” December 2012.
- [140] A. Maitra, S. Rajagopalan, J.-S. Lai, M. DuVall, and M. McGranaghan, “Medium voltage stand alone dc fast charger,” May 30 2013, uS Patent App. 13/479,389 .
- [141] J. Lai, W. Lai, S. Moon, L. Zhang, and A. Maitra, “A 15-kv class intelligent universal transformer for utility applications,” in *2016 IEEE Applied Power Electronics Conference and Exposition (APEC)*, March 2016, pp. 1974–1981.
- [142] S. Srdic, C. Zhang, X. Liang, W. Yu, and S. Lukic, “A sic-based power converter module for medium-voltage fast charger for plug-in electric vehicles,” in *2016 IEEE Applied Power Electronics Conference and Exposition (APEC)*, March 2016, pp. 2714–2719.
- [143] M. Vasiladiotis and A. Rufer, “A modular multiport power electronic transformer with integrated split battery energy storage for versatile ultrafast ev charging stations,” *IEEE Transactions on Industrial Electronics*, vol. 62, no. 5, pp. 3213–3222, May 2015.
- [144] C. Zhu. High-efficiency, medium-voltage-input, solid-state-transformer-based 400-kw/1000-v/400-a extreme fast charger for electric vehicles. [Online]. Available: https://www.energy.gov/sites/prod/files/2019/06/f64/elt241_zhu_2019_o_4.24_9.31pm_jl.pdf
- [145] S. Srdic, X. Liang, C. Zhang, W. Yu, and S. Lukic, “A sic-based high-performance medium-voltage fast charger for plug-in electric vehicles,” in *2016 IEEE Energy Conversion Congress and Exposition (ECCE)*, Sep. 2016, pp. 1–6.
- [146] X. Liang, C. Zhang, S. Srdic, and S. M. Lukic, “Predictive control of a series-interleaved multicell three-level boost power-factor-correction converter,” *IEEE Transactions on Power Electronics*, vol. 33, no. 10, pp. 8948–8960, Oct 2018.
- [147] D. Rothmund, G. Ortiz, and J. W. Kolar, “Sic-based unidirectional solid-state transformer concepts for directly interfacing 400v dc to medium-voltage ac distribution systems,” in *2014 IEEE 36th International Telecommunications Energy Conference (INTELEC)*, Sep. 2014, pp. 1–9.
- [148] D. Sha, G. Xu, and Y. Xu, “Utility direct interfaced charger/discharger employing unified voltage balance control for cascaded h-bridge units and decentralized control for cf-dab modules,” *IEEE Transactions on Industrial Electronics*, vol. 64, no. 10, pp. 7831–7841, Oct 2017.
- [149] X. She, X. Yu, F. Wang, and A. Q. Huang, “Design and demonstration of a 3.6-kv-120-v/10-kva solid-state transformer for smart grid application,” *IEEE Transactions on Power Electronics*, vol. 29, no. 8, pp. 3982–3996, Aug 2014 .
- [150] F. Wang, G. Wang, A. Huang, W. Yu, and X. Ni, “Design and operation of a 3.6kv high performance solid state transformer based on 13kv sic mosfet and jbs diode,” in *2014 IEEE Energy Conversion Congress and Exposition (ECCE)*, Sep. 2014, pp. 4553–4560.
- [151] D. Rothmund, T. Guillod, D. Bortis, and J. W. Kolar, “99.1% efficient 10 kv sic-based medium-voltage zvs bidirectional single-phase pfc ac/dc stage,” *IEEE Journal of Emerging and Selected Topics in Power Electronics*, vol. 7, no. 2, pp. 779–797, June 2019.
- [152] —, “99% efficient 10 kv sic-based 7 kv/400 v dc transformer for future data centers,” *IEEE Journal of Emerging and Selected Topics in Power Electronics*, vol. 7, no. 2, pp. 753–767, June 2019.
- [153] “Ieee recommended practice and requirements for harmonic control in electric power systems,” *IEEE Std 519-2014 (Revision of IEEE Std 519-1992)*, pp. 1–29, June 2014 .
- [154] “Ieee standard for general requirements for dry-type distribution and power transformers,” *IEEE Std C57.12.01-2015 (Revision of IEEE Std C57.12.01-2005)*, pp. 1–52, Feb 2015 .
- [155] “Electromagnetic compatibility (emc) - part 2-12: Environment - compatibility levels for low-frequency conducted disturbances and signalling in public medium-voltage power supply systems,” *IEC 61000-2-12:2003*, pp. 1–55, April 2003 .
- [156] “Electromagnetic compatibility (emc) - part 3-6: Limits - assessment of emission limits for the connection of distorting installations to mv, hv and ehv power systems,” *IEC TR 61000-3-6:2008*, pp. 1–58, February 2008 .